Quaternary Research
Copyright © University of Washington. Published by Cambridge University Press, 2021.
doi:10.1017/qua.2020.112

Oldest Dryas hydroclimate reorganization in the eastern Iberian Peninsula after the iceberg discharges of Heinrich Event 1

Carlos Pérez-Mejías[a]*, Ana Moreno[b], Juan Bernal-Wormull[b], Isabel Cacho[c], M. Cinta Osácar[d], R. Lawrence Edwards[e], Hai Cheng[a,f,g]

[a]Institute of Global Environmental Change, Xi'an Jiaotong University, 710049 Xi'an, China
[b]Department of Geoenvironmental Processes and Global Change, Pyrenean Institute of Ecology–CSIC, Avda. Montañana 1005, 50059 Zaragoza, Spain
[c]Department of Dinàmica de la Terra i de l'Oceà, Universitat de Barcelona. C/Martí Franques s/n, 08028 Barcelona, Spain
[d]Earth Sciences Department, University of Zaragoza, C/Pedro Cerbuna 12, 50009 Zaragoza, Spain
[e]Department of Earth and Environmental Sciences, University of Minnesota, 116 Church Street SE, Minneapolis, Minnesota 55455, USA
[f]State Key Laboratory of Loess and Quaternary Geology, Institute of Earth Environment, Chinese Academy of Sciences, 710049 Xi'an, China
[g]Key Laboratory of Karst Dynamics, MLR, Institute of Karst Geology, CAGS, Guilin, China
*Corresponding author at: Institute of Global Environmental Change, Xi'an Jiaotong University, Xi'an 710049, China.
Email address: perezmegias@mail.xjtu.edu.cn.

(Received April 24, 2020; Accepted October 23, 2020)

Abstract

This study examines the first precisely dated and temporally highly resolved speleothem record from Iberia that reconstructs the Oldest Dryas (OD). The onset of cold conditions in the study area, contemporary with the beginning of Heinrich Stadial 1, is recorded at 18.13 ± 0.08 ka, with a pronounced drop of 6.1‰ in $\delta^{13}C$ in 250 years. Henceforth, stadial conditions depict a period of instability in the Atlantic Meridional Overturning Circulation, peaking in freshwater input from iceberg melting during Heinrich Event 1. Anomalies in the $\delta^{18}O$ of the stalagmite attributed to such a freshwater event are found from 16.17 to 15.89 ka. Such absolute dates given to the onset of the OD in Iberia and to the main iceberg discharges are reliable anchor points for non-absolute chronologies. Two periods are identified in the OD: OD-a (18.13–16.17 ka) is characterized by wet conditions and a faster growth rate, and OD-b (15.89–14.81 ka) exhibits relative dryness and a slower growth rate. The sudden release of fresh water is considered to be the reason for the disruption of rainfall patterns in eastern Iberia. The present study also highlights the existence of heterogeneous and complex hydrological conditions during the OD in Iberia when both Atlantic and Mediterranean realms are considered.

Keywords: Speleothem; Deglaciation; Heinrich Stadial 1; Oldest Dryas; Iberia; Western Mediterranean; Atlantic Meridional Overturning Circulation

INTRODUCTION

Heinrich events were identified during the last glacial period as enhanced ice-rafted debris (IRD) that were found in marine deep sea sediments from the North Atlantic as a result of massive iceberg calving (Heinrich, 1988; Hemming, 2004). The icebergs led to huge volumes of ice rafting across the North Atlantic, leading to important changes in oceanic circulation, such as the reduction in the North Atlantic Deep Water formation (Hemming, 2004) and the consequent slowdown of the Atlantic Meridional Overturning Circulation (AMOC). In the 1990s, the slowdown of the AMOC during Heinrich events and the associated cooling in the Northern Hemisphere were attributed to the meltwater pulses from the events themselves (Broecker, 1994; Paillard and Labeyrie, 1994; Rahmstorf, 1994). However, in the 2000s, an increasing number of studies suggested that the AMOC disruption occurred before the iceberg discharges (Roche et al., 2004; Hall et al., 2006). The relationship between the North Atlantic Deep Water, the AMOC, and the oceanic changes responsible for destabilizing grounded ice shelves remained elusive until the findings of Marcott (2011) and Álvarez-Solas et al. (2011). Since these studies, a marine subsurface warming occurring at the same time as large reductions in the AMOC was identified more than 1 ka prior to a Heinrich event (Marcott et al., 2011). Here, it is worth noting the

Cite this article: Pérez-Mejías, C., Moreno, A., Bernal-Wormull, J., Cacho, I., Osácar, M. C., Edwards, R. L., Cheng, H. 2021. Oldest Dryas hydroclimate reorganization in the eastern Iberian Peninsula after the iceberg discharges of Heinrich Event 1. *Quaternary Research* 101, 67–83. https://doi.org/10.1017/qua.2020.112

Downloaded from https://www.cambridge.org/core. University of Minnesota Libraries, on 25 Aug 2021 at 21:56:09, subject to the Cambridge Core terms of use, available at https://www.cambridge.org/core/terms. https://doi.org/10.1017/qua.2020.112

clear distinction between Heinrich stadials and Heinrich events. A Heinrich stadial, characterized by low Northern Hemisphere temperatures linked to a weak AMOC, precedes a Heinrich event, which is limited to the IRD from iceberg calving recorded in the North Atlantic sediments. Recognizing that the icebergs arrived too late to trigger the initial cooling, this paradigm implies that while fresh water derived from melting ice provides a positive feedback system to prolong stadial conditions, it is not a trigger for a stadial event (Álvarez-Solas et al., 2013; Barker et al., 2015).

Together with Heinrich events, the global picture of abrupt climate changes during the last glacial cycle cannot be completed without mentioning the Dansgaard-Oeschger oscillations. Contrary to Heinrich events, which are identified in marine records, Dansgaard-Oeschger cycles are identified in Greenland ice cores and are characterized by abrupt warmings (interstadials) followed by more gradual coolings (stadials) (Dansgaard et al., 1982, 1993). Dansgaard-Oeschger variations in the North Atlantic sea surface temperatures are well correlated with Greenland temperatures, although Heinrich events are not seen with extreme low temperatures in the ice cores (Bond et al., 1999; Hemming, 2004).

The climatic response of Iberia and its surroundings to Heinrich events has been identified in several paleorecords in the last two decades (e.g., Cacho et al., 1999; Sánchez Goñi et al., 2000; Moreno et al., 2002). Marine records analyzing such oscillations are abundant in the Bay of Biscay, the Iberian margin, the Alborán Sea, and the western Mediterranean (Combourieu Nebout et al., 2002; Sánchez Goñi et al., 2002; Roucoux et al., 2005; Sierro et al., 2005; Voelker et al., 2006; Beaudouin et al., 2007; Naughton et al., 2007; Fletcher and Sánchez Goñi, 2008; Frigola et al., 2008; Toucanne et al., 2008). In contrast, the terrestrial response is not well constrained owing to the lack of good records and the problems associated with obtaining a reliable chronology (see the review of Moreno et al., 2012). Focusing on the last deglaciation, it should be noted the dearth of speleothems in Europe, specifically in Iberia (Atsawawaranunt et al., 2018; Lechleitner et al., 2018). The OD, corresponding to the counterpart of Heinrich Stadial 1 (HS-1) on the continent (Naughton et al., 2007), has been identified as the last cold event before deglaciation, and was even colder than the last glacial maximum according to some Iberian records (Cacho et al., 2001).

Regionally, records covering the OD are scarce and offer only a sparse view of cold/dry conditions (Valero-Garcés et al., 1998; González-Sampériz et al., 2006; Millet et al., 2012). Such records from the Pyrenees in northeastern Iberia exhibit rather homogeneous climate conditions during the OD, which are explained either by the location at high altitude with persistent cold conditions or by the low temporal resolution. Likewise, a stalagmite record from northern Iberia that was growing during the last glacial maximum records a hiatus in the OD (Moreno et al., 2010). Notably, an advance of the glaciers has been recorded during the OD in many mountains in Iberia (Palacios et al., 2017a, 2017b), entailing the most remarkable readvance since the last glacial maximum. Therefore, while the dominance of cold conditions is certain during the OD, inferring predominant dryness remains controversial. Because of such contradictory results, new records are needed to test the hypothesis of widespread dryness during the OD.

Some studies suggest a multiphase evolution in the hydrology in this regard; a transition from humid to dry conditions throughout the OD has been inferred by means of salinity in Lake Estanya in the Pyrenees (Morellón et al., 2009). Furthermore, the most illustrative and detailed insights about the complex structure of the OD in Iberia throughout several hydroclimate phases have been pointed out by Naughton et al., (2007, 2009, 2016), using pollen assemblies in marine cores from the Iberian margin. A tri-phase pattern was established in a few sequences with extremely high sedimentation rates, whereas two phases were detected in lower resolution sequences (Naughton et al., 2016). A pattern of wet conditions during the first (older) phase and dry conditions in the second (followed by another relatively wet phase in the case of three-folded records) is common in these records. Similar complex patterns during that period have also been reported from lake sequences and speleothems from other regions outside Iberia (Broecker and Putnam, 2012; Stríkis et al., 2015). Reconstructing the hydrological evolution during the OD in terrestrial Iberia is important to understanding the response on land to the complex climatic patterns during this event and the teleconnections established with atmospheric and oceanic processes.

Here, we present a new speleothem record from Meravelles cave in northeastern Iberia that extends across the OD. Chronologically well-resolved, the outstanding resolution reached on the stable isotopes enables the identification of decadal abrupt events in the last deglaciation. Our data suggest a heterogeneous pattern in the hydrology, with generally wetter conditions than shown in many other reconstructions of the OD in Iberia. Notably, this record shows clear shifts in $\delta^{18}O$ and $\delta^{13}C$ that are attributed to two key events: (1) the onset of the cold conditions of the OD ascribed to HS-1, and (2) the iceberg discharge in the Atlantic Ocean due to Heinrich Event 1 (HE-1) (sensu stricto). Such findings confirm the hypothesis of Álvarez-Solas et al. (2011) on a terrestrial European record.

STUDY AREA

Meravelles cave (40°56′55.62″N, 0°30′45.59″E, 125 m asl) (Fig. 1) is located in northeastern Spain, near the village of Benifallet, Tarragona. It is in the Serra de Cardó mountainous system, next to the Ebro River and 25 km from the Mediterranean Sea. It formed in lower Jurassic limestone, dolostone, and breccia, and has 510 m of mainly flat galleries, reaching a maximum depth of only 10 m (Fig. 2). Surrounding the cave is sclerophyll vegetation composed mainly of calcicole shrublands of Rosmarino-Ericion multiflorae and other taxa, including Fabaceae (*Anthyllis cytisoides*), Poaceae (*Phlomido lychnitidis-Brachypodietum retusi*), and sparse *Pinus halepensis* forests.

The local climate is typical Mediterranean (Csa following Köppen-Geiger). From 2000 to 2015, the weather station

Downloaded from https://www.cambridge.org/core. University of Minnesota Libraries, on 25 Aug 2021 at 21:56:09, subject to the Cambridge Core terms of use, available at https://www.cambridge.org/core/terms. https://doi.org/10.1017/qua.2020.112

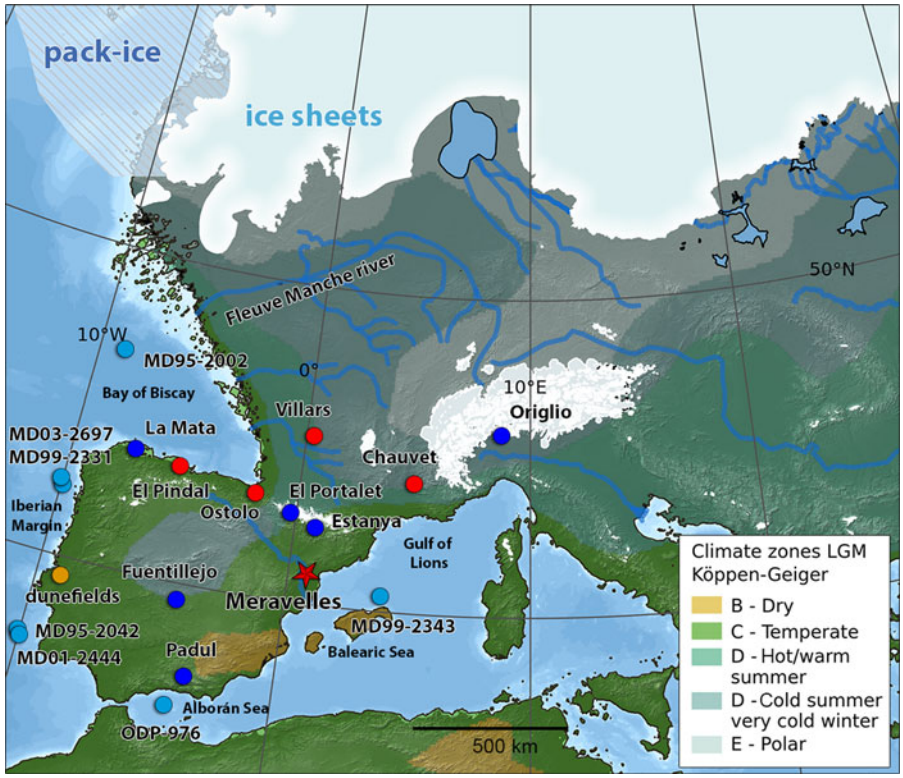

Figure 1. Paleoenvironmental reconstruction of western Europe prior to deglaciation. The sea level is -120 m compared to the modern level, according to reconstructions of the last glacial maximum. Meravelles cave (this study, red star) and other records cited in the text are indicated by the following colors: red (cave), sky blue (marine core), navy blue (lake), and yellow (dune fields, including the Caparica clifftop dune, the inland extension of the Aeolian system, and the Apostica transgressive dune field) (modified from Becker et al., 2015). (For interpretation of the references to color in this figure legend, the reader is referred to the web version of this article.)

belonging to the Global Network of Isotopes in Precipitation in nearby Tortosa measured a mean annual rainfall of 520 mm and a mean annual temperature of 18.3°C (Rodríguez-Arévalo et al., 2011). Seasonally, mean temperatures reach 26.8°C during summer and 12.0°C during winter. The hydroclimate is characterized by equinoctial rains during autumn and spring, generally dry summers, and relatively dry winters. However, it is worth noting the recurrence of episodes of high

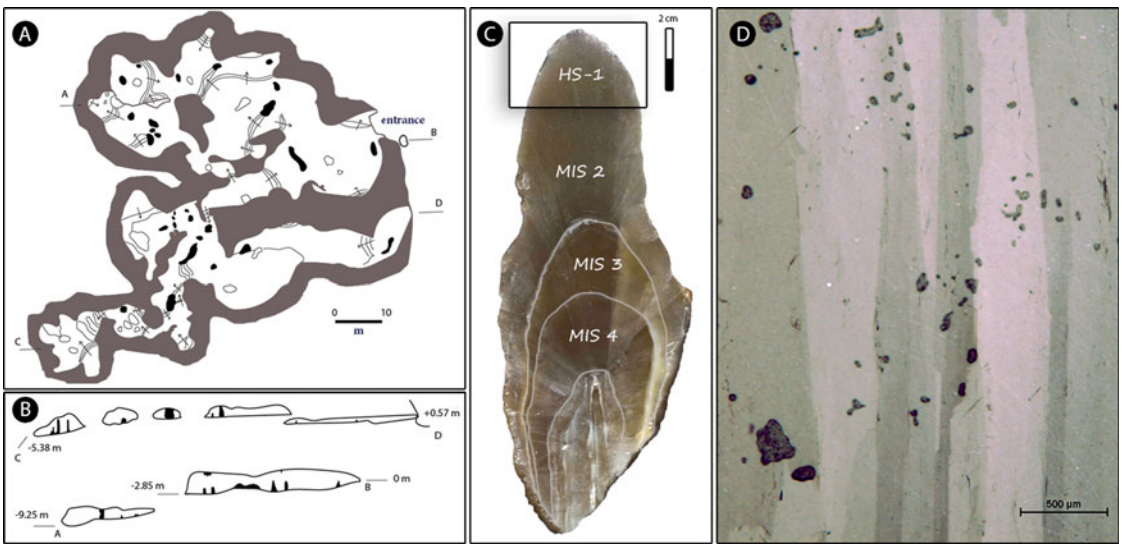

Figure 2. (color online) (A) Plan view of Meravelles cave. (B) Cross section of the cave. (C) Polished half of the MAAT record; the square at the top indicates the part of the stalagmite used in this study; some main hiatus throughout the record (gray lines) are also marked. (D) Photomicrograph showing columnar calcite fabrics.

Downloaded from https://www.cambridge.org/core. University of Minnesota Libraries, on 25 Aug 2021 at 21:56:09, subject to the Cambridge Core terms of use, available at https://www.cambridge.org/core/terms. https://doi.org/10.1017/qua.2020.112

rainfall in short intervals of time, associated with cutoff lows and mesoscale convective systems that occur mainly at the end of summer and the onset of autumn. Such episodes of extreme rainfall lead to unusually humid late summers in the year of occurrence. This was the case in 2006, 2009, and 2014 in Tortosa, where >100 mm of rainfall was recorded in September of each year. Such an amount represents 38, 45, and 21% of the total rainfall in 2006, 2009, and 2014, respectively. It must be noted that the mean rainfall during September represents only 13% of the total in the same period (Rodríguez-Arévalo et al., 2011). There is thus a subdecadal occurrence of such extreme events.

A previous study have linked the rainfall in Tortosa with the Western Mediterranean Oscillation, a low-frequency index of pressure differences between Padua (northern Italy) and San Fernando (southern Iberia) (Martin-Vide and Lopez-Bustins, 2006). In that study, rainfall data from 1951 to 2000 were compared with the Western Mediterranean Oscillation index and showed that 69.8% of rainfall events occurred under negative values in the index. This relationship is much stronger if we take into account the episodes of torrential rainfall: 96.1% of daily rainfall >50 mm coincided with a negative Western Mediterranean Oscillation index, and 100% coincided with amounts >100 mm for the same period (Martin-Vide and Lopez-Bustins, 2006).

METHODS

The stalagmite studied here (dubbed MAAT) from Meravelles cave is 15 cm long (in the present work, we focused on the top 2.5 cm, covering early deglaciation) and was collected in situ and cut along the growth axis with a diamond saw and then polished (Fig. 2). A total of 250 samples were drilled along the extension axis at 0.1-mm increments for stable isotope analysis; 26 samples were taken at 1-mm increments for trace-metal analysis, and 14 samples were taken for ^{230}Th dating at different intervals, mainly every 1–2 mm, to identify any potential change in growth rate. A thin section covering the whole area of MAAT was examined using transmitted light microscopy.

Stable isotopes analysis was performed at the Isotope Laboratory of Xi'an Jiaotong University, using a ThermoFisher Delta V Plus mass spectrometer coupled with a Kiel-IV. Values are reported as $\delta^{18}O$ (‰) and $\delta^{13}C$ (‰) with respect to the Vienna Pee Dee Belemnite (VPDB) standard. Long-term precision for $\delta^{13}C$ and $\delta^{18}O$ (1σ) was 0.03 and 0.06‰, respectively. Calibration of the raw results versus the VPDB scale was achieved using TTB-1 and NBS 18 reference materials. Trace metal analysis was performed at the Pyrenean Institute of Ecology, using inductively coupled plasma-optical emission spectrometry (ThermoFisher iCAP DUO 6300). An approximate 1-mg sample was dissolved in 2% HNO_3. The results were expressed as molar ratios against Ca. ^{230}Th dating was performed using a Thermo Neptune multicollector inductively coupled plasma mass spectrometer at Xi'an Jiaotong University and the University of Minnesota, following the methodology described in Cheng et al. (2000). The decay constants are reported in Cheng et al. (2013).

The depth-age model was constructed using COPRA (Breitenbach et al., 2012), tracing the confidence interval (95%) through Monte Carlo simulations by the PHCIP method with the 2σ deviation from the median trajectory of the proxy. The ages are expressed in years before present (BP). Spectral analyses were run in REDFIT (Schulz and Mudelsee, 2002) and Morlet continuous wavelet in Matlab (Grinsted et al., 2004), with time series interpolated at equal steps. All the correlations used in this study were calculated with Spearman's rank correlation coefficient (ρ).

RESULTS

Petrography, age model, and growth rate

Focusing on the top 2.5 cm of MAAT, long and thin crystals parallel to the growth axis were identified, with a length/width ratio >6:1 and flat regular borders (Fig. 2). Thin-section observation suggests that the sample is entirely composed of calcite. The fabric corresponds to "columnar," following the nomenclature of Frisia (2015). Neither macro- nor microlamination was recognized in the sample.

A total of 14 ^{230}Th dates (Table 1) extracted from the top 2.5 cm of MAAT were used to build the chronological record (Fig. 3a), showing mean analytical uncertainties of 3‰. Samples are genuinely clean, reaching consistent and high ^{230}Th/^{232}Th ratios between 2000 and 25,000 (Table 1). ^{238}U content is approximately 460 parts per billion (ppb), whereas $\delta^{234}U_{initial}$ is approximately 400 (Table 1).

Growth rate ranges from 1 to 2 µm/yr (15.71–15.27 ka), 31 to 32 µm/yr (18.49–18.47 ka), and 20 to 21 µm/yr (17.85–17.81 ka) (Fig. 3b). Mean growth rate is 12 µm/yr. Focusing on key events, growth rates are approximately 4 µm/yr during the onset of the OD (18.13 ka), whereas 6–4 µm/yr are reached during the $\delta^{18}O$ negative anomaly in the main part of the OD (16.17–15.89 ka). The continuous growth of MAAT during the OD is remarkable, given other regional cave records, such as Villars cave (Genty et al., 2006) and El Pindal (Moreno et al., 2010), exhibit hiatus during this event.

Isotope and trace-metal geochemistry

The $\delta^{18}O$ record of MAAT shows values between −5.84 and −3.75‰ (mean = −4.70 ± 0.02‰). The lowest $\delta^{18}O$ values are reached in the bottom part of the record (18.47 ka), while the maximum occurred at 16.02 ka (Fig. 3c). The $\delta^{13}C$ values range from −8.27 to + 1.74‰ (mean = −2.30 ± 0.22‰). Similar to $\delta^{18}O$, the lowest $\delta^{13}C$ values are found in the oldest part of the record (18.61 ka), while the highest are reached at 15.49 ka (Fig. 3d). The absolute $\delta^{13}C$ variability is notably high, reaching a 10.01‰ in a 4-ka-long record. Interestingly, $\delta^{18}O$ and $\delta^{13}C$ are well correlated (ρ = 0.66, p-value <0.001) throughout the record. The temporal resolution reached on the stable isotope data varies between 4 and 71 years, with an average resolution of 16 years. The

Downloaded from https://www.cambridge.org/core. University of Minnesota Libraries, on 25 Aug 2021 at 21:56:09, subject to the Cambridge Core terms of use, available at https://www.cambridge.org/core/terms. https://doi.org/10.1017/qua.2020.112

Table 1. ^{230}Th dating results.

Sample name	^{238}U (ppb)[a]	^{232}Th (ppt)[b]	^{230}Th/^{232}Th (atomic × 10^{-6})	δ^{234}U[c] (measured)	^{230}Th/^{238}U (activity)	^{230}Th age (yr) (uncorrected)	$\delta^{234}U_{initial}$[d] (corrected)	^{230}Th age (yr BP) (corrected)[e]
MAA-0.5	249.2 ± 0.2	316 ± 6	2,287 ± 46	368.6 ± 1.5	0.1756 ± 0.0005	14,885 ± 50	384 ± 2	14,789 ± 54
MAA-2.0	328.3 ± 0.2	46 ± 13	21,197 ± 5794	376.2 ± 1.5	0.1807 ± 0.0004	15,253 ± 38	393 ± 2	15,181 ± 38
MAA-3.0	430.0 ± 1.0	320 ± 6	4,148 ± 85	372.1 ± 1.6	0.1869 ± 0.0004	15,862 ± 44	389 ± 2	15,782 ± 45
MAA-5.0	475.9 ± 0.3	184 ± 4	8,241 ± 166	388.9 ± 1.0	0.1937 ± 0.0004	16,271 ± 35	407 ± 1	16,194 ± 35
MAA-6.5	509.3 ± 0.5	103 ± 12	16,157 ± 1845	391.6 ± 1.6	0.1974 ± 0.0003	16,565 ± 38	410 ± 2	16,492 ± 38
MAA-8.5	469.9 ± 0.4	133 ± 8	11,888 ± 684	401.4 ± 1.6	0.2045 ± 0.0004	17,078 ± 39	421 ± 2	17,004 ± 39
MAA-9.5	470.4 ± 0.4	295 ± 6	5,512 ± 111	418.8 ± 1.6	0.2097 ± 0.0004	17,307 ± 43	440 ± 2	17,225 ± 44
MAA-11.5	590.9 ± 0.7	981 ± 20	2,097 ± 42	394.6 ± 1.8	0.2111 ± 0.0005	17,765 ± 50	415 ± 2	17,667± 56
MAA-14.0	434.5 ± 0.5	181 ± 8	8,291 ± 351	372.3 ± 1.6	0.2091 ± 0.0004	17,899 ± 45	392 ± 2	17,821 ± 46
MAA-16.0	313.7 ± 0.3	54 ± 1	20,009 ± 403	361.9 ± 1.4	0.2084 ± 0.0005	17,978 ± 50	381 ± 1	17,905 ± 50
MAA-18.0	448.3 ± 0.6	188 ± 4	8,363 ± 171	358.5 ± 1.7	0.2122 ± 0.0005	18,388 ± 54	378 ± 2	18,315 ± 55
MAA-20.0	324.0 ± 0.4	96 ± 7	11,857± 893	349.8 ± 1.6	0.2125 ± 0.0005	18,541 ± 54	369 ± 2	18,465 ± 54
MAA-22.5	336.2 ± 0.3	46 ± 6	25,836 ± 3620	353.4 ± 1.5	0.2136 ± 0.0004	18,594 ± 45	372 ± 2	18,522 ± 45
MAA-25.0	338.2 ± 0.3	91 ± 2	13,103 ± 264	354.8 ± 1.4	0.2148 ± 0.0005	18,683 ± 50	374 ± 1	18,609 ± 50

Note: The error is 2σ. Sample name numbers refer to the distance in millimeters from the top.
[a]ppb = parts per billion.
[b]ppt = parts per trillion.
[c]$\delta^{234}U = ([^{234}U/^{238}U]_{activity} - 1) \times 1000$.
[d]$\delta^{234}U_{initial}$ was calculated based on the ^{230}Th age (T); i.e., $\delta^{234}U_{initial} = \delta^{234}U_{measured} \times e^{\lambda 234 \times T}$.
[e]Corrected ^{230}Th ages assume the initial ^{230}Th/^{232}Th atomic ratio of $4.4 \pm 2.2 \times 10^{-6}$. Those are the values for a material at secular equilibrium, with the bulk earth ^{232}Th/^{238}U value of 3.8. The errors are arbitrarily assumed to be 50%.

subdecadal resolution is reached during 18.6–18.3 and 17.9–17.7 ka.

The trace-metal ratios analyzed, namely Mg/Ca and Sr/Ca, show a statistically significant strong positive correlation (ρ = 0.9, p-value <0.001) throughout the record. The lowest values in both stable isotope and trace-metal ratios are reached in the oldest part of the record; the highest values are seen in the youngest section.

DISCUSSION

Interpretation of proxies

$\delta^{18}O$

The columnar fabric of MAAT, considered a primary fabric, is likely associated with near-equilibrium conditions during the formation of the speleothem (Frisia et al., 2000, 2018). The correct stratigraphic order of the ^{230}Th dates and the absence of diagenetical evidence support the primary origin of the fabric.

When a positive correlation between $\delta^{18}O$ and $\delta^{13}C$ is found in speleothems, it might be considered evidence of isotopic disequilibrium (Mickler et al., 2006). Kinetic effects, such as rapid CO_2 degassing, and evaporative effects in the cave, would lead to an enrichment of speleothem ^{18}O and ^{13}C (Wiedner et al., 2008). However, some recent reviews highlight the existence of positive correlations between speleothem $\delta^{18}O$ and $\delta^{13}C$ in many paleoclimate studies (Fairchild et al., 2006; Mickler et al., 2006). Indeed, such correlation may respond to environmental factors when $\delta^{18}O$ and $\delta^{13}C$ variability is controlled by rainfall amount and vegetation activity, respectively. In the Mediterranean, many examples of stalagmites sensitive to changes in rainfall amount also show positive correlation between $\delta^{18}O$ and $\delta^{13}C$ without their respective paleoclimate relevance being compromised (e.g., Drysdale, 2006; Columbu et al., 2017; Regattieri et al., 2018).

Once diagenetic processes are discarded, $\delta^{18}O$ of speleothems from mid-latitudes are driven by several factors that in turn control the $\delta^{18}O$ of the precipitation, such as cloud condensation temperature (Dansgaard, 1964; Fricke and O'Neil, 1999), storm track pathways (Sturm et al., 2007), variations in the ocean water $\delta^{18}O$ (Schrag et al., 2002), changes in the vapor source (Charles et al., 1994), changes in seasonality (Denton et al., 2005), and amount of rainfall (Rozanski et al., 1993). In the present record, changes in the vapor source are not expected owing to the orography of the study area, leeward of the Atlantic influence and hydrologically controlled by rainfall of Mediterranean origin. Different storm track pathways might occasionally affect $\delta^{18}O$ at event—or even monthly—scale, but it is unlikely at the millennial scale of this study with a prevalent zonal atmospheric circulation that characterized glacial stages (Li and Battisti, 2008; Beghin et al., 2015).

The meltwater discharges mainly during spring and summer decrease the AMOC and preclude the northward oceanic heat transfer, expanding sea-ice cover in the North Atlantic, including the Bay of Biscay (Zaragosi et al., 2001), and setting the climate in a winter-centric mode (Denton et al., 2005, 2010; Toucanne et al., 2015). In a deglaciation in "apparent" cold conditions (Toucanne et al., 2015), halfway through the precession cycle, changes in rainfall seasonality are unlikely to exert an important role on $\delta^{18}O$ variability.

Downloaded from https://www.cambridge.org/core. University of Minnesota Libraries, on 25 Aug 2021 at 21:56:09, subject to the Cambridge Core terms of use, available at https://www.cambridge.org/core/terms. https://doi.org/10.1017/qua.2020.112

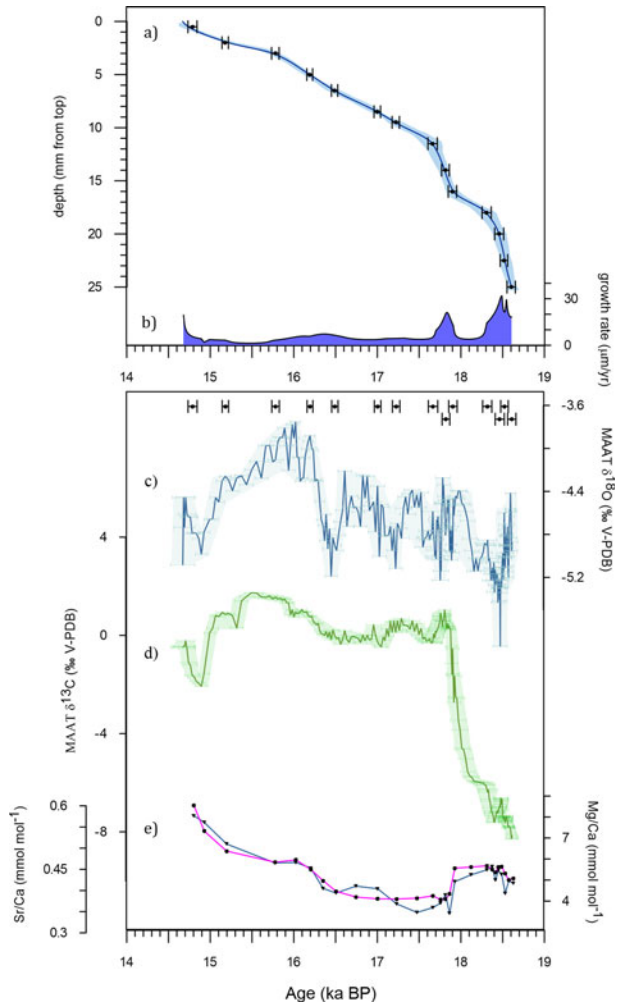

Figure 3. Results from the MAAT record. (a) Age model. (b) Growth rate. (c) $\delta^{18}O$. (d) $\delta^{13}C$. (e) Mg/Ca (= pink) and Sr/Ca (= blue) trace-metal ratios. ^{230}Th dates with uncertainties are also indicated. (For interpretation of the references to color in this figure legend, the reader is referred to the web version of this article.)

An isotopic analysis of rainfall samples from the Tortosa weather station (Rodríguez-Arévalo et al., 2011) establishes a $\delta^{18}O$-T relationship of 0.27‰ $°C^{-1}$. This slope is slightly higher than the cave fractionation factor, of negative sign (Kim and O'Neil, 1997; Tremaine et al., 2011), but clearly not of enough amplitude to offer a good signal-to-noise ratio. Besides, in the same dataset, the relationship between the $\delta^{18}O$ of the precipitation and amount of rainfall is –1.6‰ per 100 mm/month. Similar gradients in temperature and amount effect have been reported from the central and western Mediterranean (Regattieri et al., 2018), but the calculated gradients are site- and time-specific. Its use should be taken with care, and direct inferences of such values in the deglaciation are controversial.

Looking in more detail at the MAAT record, the trend to a lower $\delta^{18}O$ through the end of the OD to the onset of the Bølling (Fig. 3) is unlikely to be explained by changes in air temperature, that would be attributed to cold conditions if that would be the interpretation of the $\delta^{18}O$. At the same time, the apparent sensitivity of $\delta^{13}C$ to changes in temperature (see "$\delta^{13}C$ and trace-metal ratios" section below) would not be followed by any interpretation of $\delta^{18}O$ variability as representative of such temperature changes. In this regard, especially illustrative is the jump in $\delta^{13}C$ at ~18 ka that would be marked by contradictory warm conditions with such $\delta^{18}O$ interpretation. On the contrary, high growth rates are accompanied by low $\delta^{18}O$ as well as low trace-metal ratios, suggesting a variability controlled mainly by hydrological availability. Despite that $\delta^{18}O$ variability might reflect a mixing of factors that cannot be totally ruled out, and taking into consideration the above-mentioned reasons, we suggest that the amount of rainfall drives the $\delta^{18}O$ variability in this record, being also sensitive to changes in ocean water $\delta^{18}O$. The amount of rainfall as a main control of $\delta^{18}O$ variability has been commonly reported from speleothems in the Mediterranean area; for example, in Italy (Zanchetta et al., 2007; Drysdale et al., 2009; Columbu et al., 2017), Macedonia (Regattieri et al., 2018), and Israel (Bar-Matthews et al., 2000). In this regard, MAAT is the first speleothem reported from Spain with such an unambiguous "Mediterranean pattern" in $\delta^{18}O$.

$\delta^{13}C$ and trace-metal ratios

The carbon in speleothems has two main sources: (1) soil CO_2 controlled by atmospheric CO_2, plant respiration, and organic matter degradation (usually 80–90% of the total in most temperate caves); and (2) bedrock carbonate that is dissolved during seepage (Genty et al., 2001, 2006). In other latitudes, $\delta^{13}C$ variability has been suggested as a proxy of changes in C4/C3 vegetation types (Dorale et al., 1998), but we hypothesize this is unlikely for our study area because of the lack of proper climate conditions for C4 plants to develop (Collatz et al., 1998). Other speleothems in southern France and northeastern Spain have proved to be powerful records of change in vegetation productivity, soil, and microbial activity (Genty et al., 2006; Pérez-Mejías et al., 2017).

The overall covariation between $\delta^{13}C$ and alkaline earth metal ratios is strong in the present record and suggests a common control, probably climate-related. Correlation of Mg/Ca and Sr/Ca may be explained by prior calcite precipitation, when the infiltration waters through the epikarst reached voids or areas with lower pCO_2 than that which they had previously equilibrated (Fairchild et al., 2000; Fairchild and Treble, 2009). In addition, prior calcite precipitation favors the release of ^{12}C into degassed CO_2, thus increasing ^{13}C in the dripwaters (Johnson et al., 2006). In MAAT, $\delta^{13}C$ reaches positive values during the main phase of the OD, so a minimal contribution of pedogenic carbon or extreme CO_2 degassing during that time is expected on account of the cold conditions.

We propose that the spike of 6.1‰ in $\delta^{13}C$ from 18.13 to 17.88 ka is due to the decay of vegetation and soil productivity in a context of extremely cold temperatures, thus reflecting the onset of the OD. Whereas the hydrological proxies ($\delta^{18}O$ and trace metals) suggest a turn into dry conditions at that time, it seems that it is not of enough magnitude to explain

Downloaded from https://www.cambridge.org/core. University of Minnesota Libraries, on 25 Aug 2021 at 21:56:09, subject to the Cambridge Core terms of use, available at https://www.cambridge.org/core/terms. https://doi.org/10.1017/qua.2020.112

such a dramatic decay into high $\delta^{13}C$. Hence, the most likely interpretation for such decay is the drop in temperature, in agreement with the arrival of cold conditions in oceanic records (Sierro et al., 2005; Martrat et al., 2007). It is worth noting that in semiarid regions, precipitation is usually expected to be a major factor limiting vegetation productivity (see Ait Brahim et al., 2017); during the OD, the MAAT record seems mostly conditioned by the cold temperatures instead.

Atlantic versus Mediterranean influences in Iberia: two sides of the same coin

The multiple factors influencing $\delta^{18}O$ in the hydrological cycle (Lachniet, 2009) usually complicate an unambiguous interpretation of its climatic significance in stalagmites (Genty et al., 2006, 2010; Fleitmann et al., 2009; Scholz et al., 2012; Moreno et al., 2017; Pérez-Mejías et al., 2017; Lechleitner et al., 2018). This fact acquires particular relevance in Iberia, a territory with a great diversity of climates close to one another and under the influence of two different regimes: the Atlantic and Mediterranean. Hence, some concrete geographical constraints might tilt the balance favoring a determinate parameter (e.g., temperature, amount of rainfall, changes in seasonality) to be dominant in $\delta^{18}O$ variability. Studies of stalagmites from Iberia reveal that the role of such parameters influencing $\delta^{18}O$ vary temporally as a response to long-term processes (e.g., ice volume, insolation) as well as abrupt ones (e.g., meltwater outburst during a glacial termination) (Pérez-Mejías et al., 2017, 2019).

In an attempt to disentangle Atlantic versus Mediterranean influences in Iberian records, it is helpful to compare MAAT with the contemporary speleothem record of OST-2 from Ostolo cave in northern Spain, which is under clear Atlantic influence (Figs. 1, 4). For instance, while hydrological availability is the factor that seems to drive the $\delta^{18}O$ variability of MAAT, it contrasts with the dominance of surface air temperature changes in the $\delta^{18}O$ of OST-2, as seen in the pronounced jump to higher $\delta^{18}O$ at the onset of the Bølling period (Fig. 4). OST-2 and MAAT records are inversely correlated (note the reversal axis in MAAT, Fig. 4), suggesting coeval changes related to temperature in the former and hydrology in the latter. A clear trend toward a cold (OST-2) and dry (MAAT) climate from 16.4 to 16.0 ka is noteworthy, whereas mild (OST-2) and more humid (MAAT) conditions are inferred from 15.9 to 14.7 ka. This example illustrates the complexities inherent in $\delta^{18}O$ interpretation in speleothems from this area; Meravelles and Ostolo caves are only about 325 km apart but are in different geographical settings and thus have a different $\delta^{18}O$ response to climatic parameters.

Therefore, the present data suggest that the OD signal in terrestrial Iberia follows a pattern of mild temperatures in locations under Atlantic influence, while wet conditions are seen in Mediterranean areas. Likewise, when cold temperatures prevail in Atlantic areas, a trend to dryness spreads in the Mediterranean. It should be noted the heterogeneity of both climate regimes during the OD regarding to temperature and hydrology. Thus, the global picture of a homogeneous cold-dry

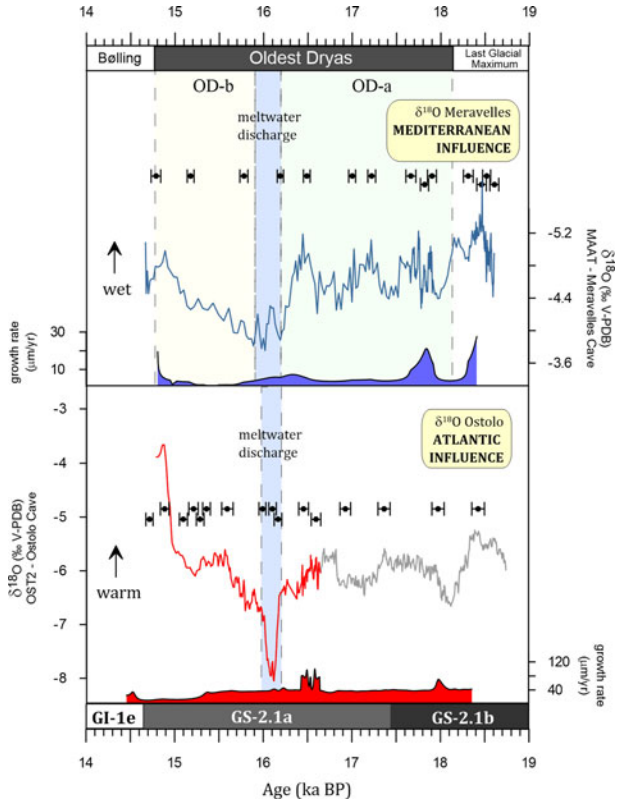

Figure 4. Comparison of MAAT (Meravelles cave; this study) (top) and OST-2 (Ostolo cave) (bottom) records showing $\delta^{18}O$ of MAAT (reversed axis) and growth rate (blue) and $\delta^{18}O$ of OST-2 and growth rate (red) (Bernal-Wormull et al., under review). ^{230}Th dates with uncertainties are also indicated. The chronology of Oldest Dryas (OD)-a and OD-b is based on MAAT; Greenland Interstadial (GI)-1e and Greenland Stadial (GS)-2.1a and GS-2.1b are based on INTIMATE chronology (Rasmussen et al., 2014). The onset of OD-a is established at 18.13 ka, since it represents the beginning of the pronounced trend into higher $\delta^{13}C$ values. (For interpretation of the references to color in this figure legend, the reader is referred to the web version of this article.)

OD throughout Iberia is not valid. Such a differentiation in the signals of speleothems may be of interest to other studies covering the last deglaciation in Iberia.

Furthermore, evidence of the change in $\delta^{18}O$ of Atlantic seawater inferred from the $\delta^{18}O$ of OST-2 at 16.2–15.9 ka (Fig. 4) is noticeable as a response to the iceberg discharge of HE-1. Similarly, we hypothesize that the excursion to lower values seen in the $\delta^{18}O$ of MAAT at that time is also the consequence of such a dramatic event. The location of Meravelles cave near the Mediterranean Sea shows that the isotopic change seen in MAAT could respond to the propagation of ^{18}O-depleted melting water through the Strait of Gibraltar to the western Mediterranean. Discarding other sources of freshwater fluxes, such as hypothetical enhanced river runoffs that are unlikely during this time, the peaks of low $\delta^{18}O$ of MAAT are presumably explained by the entrance of freshened Atlantic water. Previous records from the Mediterranean Sea suggest the arrival of such fresh water during HE-1 (Sierro et al., 2005) and few millennia before with

Downloaded from https://www.cambridge.org/core. University of Minnesota Libraries, on 25 Aug 2021 at 21:56:09, subject to the Cambridge Core terms of use, available at https://www.cambridge.org/core/terms. https://doi.org/10.1017/qua.2020.112

enhanced fluvial discharges from northern European glaciers (Bazzicalupo et al., 2018; Ausín et al., 2020). Likewise, taking into account the main assumption of $\delta^{18}O$ controlled by hydrological availability, any hypothetical increase in humid conditions at that time is unlikely to explain such $\delta^{18}O$ excursion, since it cannot be supported by trace-metal ratios or any other hydrological proxy.

The decrease of 0.42‰ in the $\delta^{18}O$ of MAAT compared to the pronounced decrease of 1.65‰ in OST-2 attributed to meltwater discharge may be explained by the latter's geographical location near the Atlantic Ocean. Hence, it is less affected by fractionation processes that might increase with distance to the source area, and it is directly influenced by changes in the water composition of the ocean. Moreover, the change in the isotopic composition of Mediterranean seawater is mitigated by the mixing of preexisting waters between different seas, with the particularity that the Mediterranean is generally ^{18}O-enriched because of higher evaporation. Quite illustrative in this respect is the higher $\delta^{18}O$ in MAAT throughout the OD compared to OST-2 (Fig. 4), suggesting different origins of the main vapor source(s) besides the contrasted air temperature between both source areas, a factor inherent in the dissimilarities between the Atlantic and Mediterranean (Pérez-Mejías et al., 2018).

Two stages in the Oldest Dryas

Based on the results of the MAAT record, we detect two different stages in the OD (OD-a from 18.13 to 16.17 ± 0.08 ka and OD-b from 15.89 to 14.81 ± 0.08 ka), supported by: (a) $\delta^{18}O$ variability, (b) trace-metal profile, (c) changes in growth rate, and (d) statistical remarks and spectral analysis. The discharge of meltwater into the Atlantic associated with HE-1 exerts as a key event delimitating the transition between both stages.

During OD-a, the mean value for $\delta^{18}O$ was −4.66‰, lower than −4.43‰ during OD-b. Likewise, alkaline earth metal ratios (Mg/Ca and Sr/Ca) exhibit lower values during OD-a and a subsequent clear trend to higher values (Fig. 3). Both $\delta^{18}O$ and metal ratios suggest a common mechanism of hydrological changes behind the variability, with relatively humid conditions in OD-a and dryness during OD-b. This hypothesis is supported by the carbonate precipitation rate, with faster growth rates when water availability is higher.

Statistical insights into the MAAT $\delta^{18}O$ time series show a stationary behavior (i.e., with no trend) during OD-a, turning to nonstationary behavior after the change in oceanic $\delta^{18}O$ due to the arrival of meltwater. Analyses of the frequencies show that the end of the multidecadal and multicentennial periodicities are found after the meltwater outburst (Fig. 5), these cycles were notably intense in frequencies of ~500 to 800 years. Similar ~500-year-cycles played an important role in the eastern Mediterranean and Asian summer monsoon intensity during the Holocene (Cheng et al., 2015; Xu et al., 2019). Likewise, the frequencies in the range of ~250–350 years, intense during late OD-a, also came to an end (Fig. 5). If we convert the time series into percentiles, the end of the frequencies is rather abrupt, suggesting a linear response to climate (Grinsted et al., 2004). Therefore, a reorganization of the oceanic currents and air masses in the Mediterranean seems to impact the cadence of rainfall in this area.

In the absence of a clear delimitation between phases, other records in northern Iberia suggest cold/dry conditions during the OD, but some of them lack a resolution good enough to explore any heterogeneous pattern and/or are under persistent climatic conditions due to the high altitude. Some examples of such conditions can be found in lake sequences from northern Iberia, with the development of steppic communities dominated by *Artemisia* and a decrease in *Pinus* percentages that characterizes La Mata sequence, Cantabrian range (Jalut et al., 2010), whereas a replacement of *Juniperus* by *Artemisia* was detected in El Portalet in the Pyrenees (González-Sampériz et al., 2006).

In central Iberia, Fuentillejo maar—also a lacustrine record—was characterized by much detrital input and erosion, low lake level, low organic productivity, and high *Juniperus* content (Vegas et al., 2010). The retreat of tree species and the development of nonarboreal species is clearly also seen in southern Iberia, inferred from the Padul sequence (Ortiz et al., 2010). In addition, pollen recovered from Mediterranean marine cores offers additional evidence of the rise in steppe taxa and reduction in arboreal communities in this area, such as the Alborán Sea (Sánchez Goñi et al., 1999, 2002; Combourieu Nebout et al., 2002, 2009; Fletcher and Sánchez Goñi, 2008) and the Gulf of Lions (Beaudouin et al., 2007). The replacement of tree species by steppe taxa has been used to model climate conditions at that time (Kageyama et al., 2005), and it has also resulted in modeling studies of vegetation types covering the whole of Iberia during the OD (Ludwig et al., 2018). Interestingly, the model of Ludwig et al. (2018) infer dry conditions in southern Iberia in contraposition to the north, a hypothesis going in the same line of proxy data and results presented here.

A close comparison with the absolute-dated speleothem record from Ostolo cave prevents any consideration about two stages in that cave with the present data (Fig. 4). Firstly, the growth rate declines in OST-2 at ~15.3 ka, which is later than the decline seen in MAAT $\delta^{18}O$ just after the meltwater discharge. Secondly, the OST-2 chronology is not well constrained prior to 16.6 ka (corresponding mostly to OD-a; see Fig. 4, gray color), so it is not possible to assess comparisons during that period. More illustrative in discerning two phases is Estanya Lake in the Pre-Pyrenees (Fig. 1), where a significant change into a more positive water balance was identified from 17.3 to 16.2 ka (Morellón et al., 2009), in agreement with more water availability identified in MAAT during OD-a. Besides, the demise of the positive water balance is rather abrupt, coinciding with HE-1 (Morellón et al., 2009) and matching the expansion of *Artemisia* in the Pyrenees (González-Sampériz et al., 2006).

The two hydrological phases of the present record (Fig. 6a, b) are in agreement with those proposed in pollen records from the MD99-2331 and MD03-2697 marine cores from the Iberian margin (Naughton et al., 2009). While the old

Downloaded from https://www.cambridge.org/core. University of Minnesota Libraries, on 25 Aug 2021 at 21:56:09, subject to the Cambridge Core terms of use, available at https://www.cambridge.org/core/terms. https://doi.org/10.1017/qua.2020.112

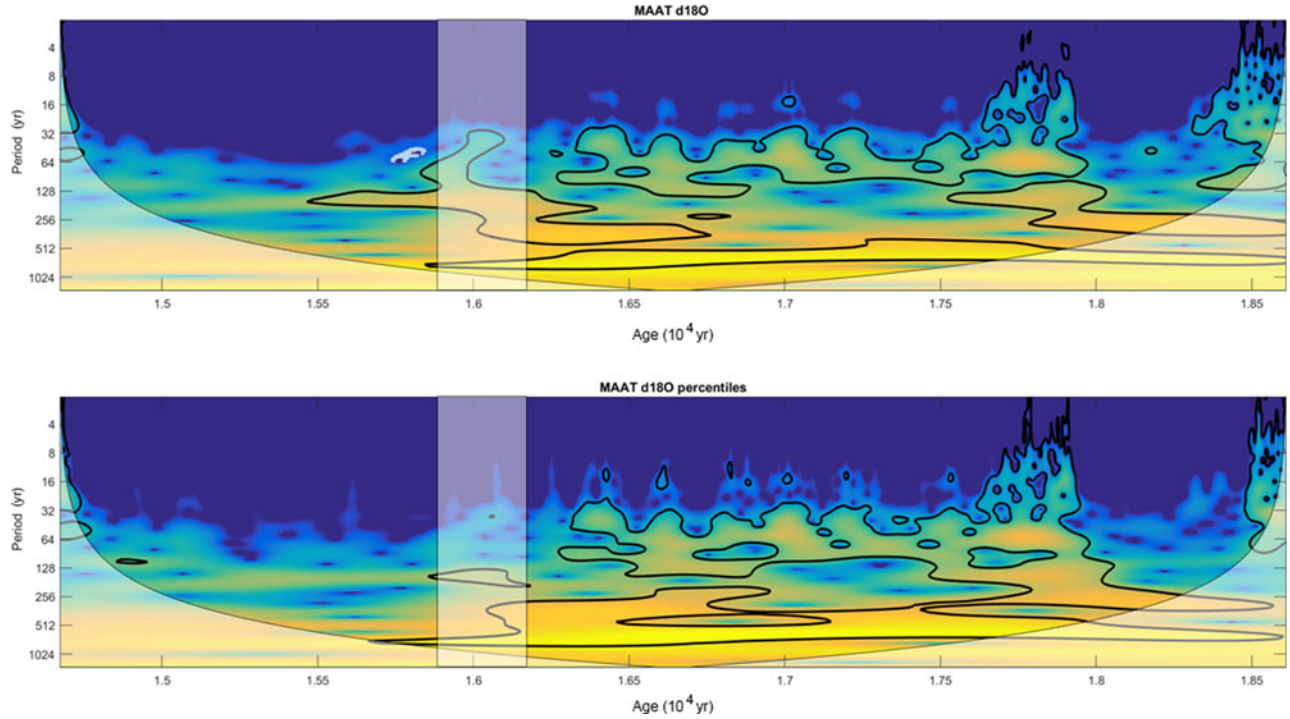

Figure 5. (color online) Analysis of frequencies of the MAAT $\delta^{18}O$ record through the Morlet continuous wavelet using absolute values (top) and percentiles (bottom). The cone of influence and the period of meltwater discharge following the chronology of the present record are also indicated.

part of the stadial is dominated by forest regression and the expansion of *Calluna vulgaris* and *Isoetes* fern (humid), the second stage shows an increase in semidesert plants (e.g., *Artemisia*) (dry) (Naughton et al., 2007). Along the same lines, such delimitation applies if we look at the temperature. The first phase is dominated by cold conditions by means of heavy $\delta^{18}O$ values of *Globigerina bulloides*, an increase in *Neogloboquadrina. pachyderma* (s.), a *Pinus* contraction, a decrease in sea surface temperatures, and an absence of IRD. The second phase is characterized by light $\delta^{18}O$ values of planktic foraminifera, *Pinus* expansion, and the presence of IRD, evidencing less cold conditions and iceberg melting in the Iberian margin (Bard et al., 2000; Naughton et al., 2009). In the Mediterranean Sea, data from foraminifera and sedimentological proxies from the MD99-2343 core (Balearic Sea) also suggest different stages (Fig. 6c, d). The first stage is characterized by an increased silt/clay ratio and a higher $\delta^{18}O$ of *G. bulloides*, signaling a weaker western Mediterranean deep water and cold conditions; the second stage presents lower silt/clay ratio and a decrease in the $\delta^{18}O$ of *G. bulloides*, reflecting a stronger western Mediterranean deep water and warmer conditions (Sierro et al., 2005; Frigola et al., 2008). Deep water sources in the Gulf of Lion depend mainly on wind variability and fluvial water discharges (Frigola et al., 2008).

In sum, the presented results, together with comparisons with many other regional marine records, suggest that the two-phase pattern in the OD seen in MAAT appears to occur synchronously despite the age model uncertainties in these marine records. Although most records (preferentially from the south) suggest dry conditions during the OD, our record implies relatively humid conditions, at least during most of OD-a. Humid conditions have also been proposed in other parts of northern Iberia, such as in the northwest (Naughton et al., 2009) and northeast (Morellón et al., 2009). Such areas match those occupied by hunter-gatherers, as inferred from the available archaeological sites. They were concentrated along the northern and eastern Iberian coast, in contrast to the south that probably was under persistent drought conditions at that time (Ludwig et al., 2018; Weniger et al., 2019).

Timing of the deglaciation in Iberia

The onset of HS-1 cannot be understood without invoking the sequence of events that happened since the end of the last glacial maximum. At ~20–18 ka, the ice retreat induced by warming started in Fennoscandia, with the consequence of enhanced freshwater fluxes into the North Atlantic, provoking a sea level rise of approximately 2 m in the Nordic Seas (Álvarez-Solas et al., 2011). The discharges of the Fleuve Manche paleoriver, interpreted by means of turbidite deposits, increased drastically at ~18.3 ka and were clearly more intense compared to the beginning of the deglaciation at ~20 ka (Toucanne et al., 2008). Such freshwater fluxes turn the ocean into a new state of weakened AMOC that precipitates the onset of HS-1 (Denton et al., 2010; Álvarez-Solas et al., 2011).

Downloaded from https://www.cambridge.org/core. University of Minnesota Libraries, on 25 Aug 2021 at 21:56:09, subject to the Cambridge Core terms of use, available at https://www.cambridge.org/core/terms. https://doi.org/10.1017/qua.2020.112

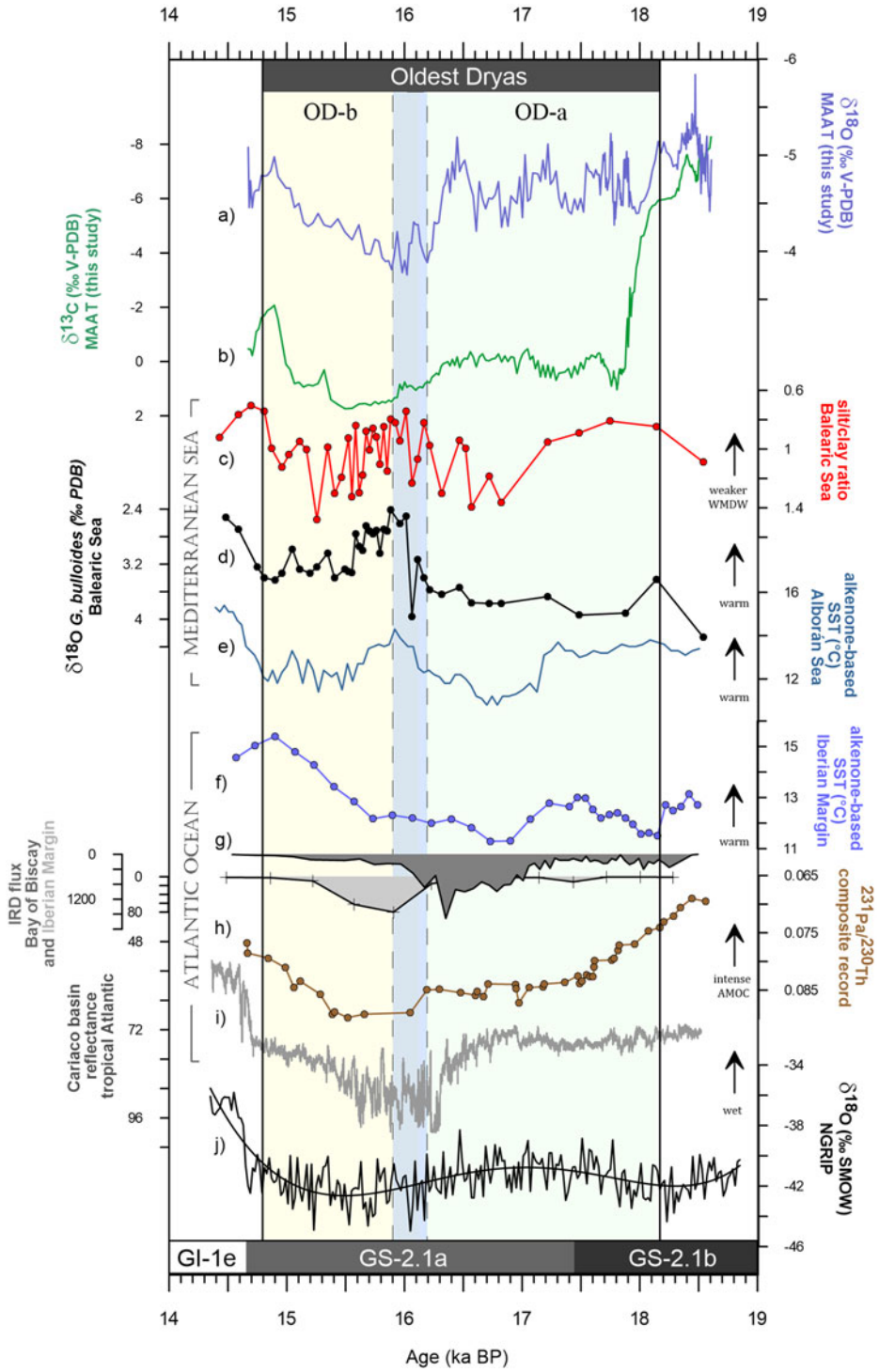

Figure 6. Comparison of global records from the Mediterranean and Atlantic realms. From top to bottom: (a) $\delta^{18}O$ of MAAT (blue) (this study) (reversed axis). (b) $\delta^{13}C$ of MAAT (green) (this study). (c) Silt/clay ratio of the noncarbonate fraction from core MD99-2343 (red) (Frigola et al., 2008). (d) $\delta^{18}O$ of *Globigerina bulloides* from core MD99-2343 (black) (Sierro et al., 2005). (e) Alkenone-based sea surface temperature reconstruction from core ODP-976 (blue) (Martrat et al., 2014). (f) Alkenone-based sea surface temperature from core MD01-2444 (blue) (Martrat et al., 2007). (g) Ice-rafted debris flux (>150 μm, %) from cores MD95-2002 (Eynaud et al., 2012) (g/cm^2/ka) and SU81-18 (gray) (Bard et al., 2000). (h) $^{231}Pa/^{230}Th$ composite record (brown) (Ng et al., 2018). (i) Reflectance in the Cariaco basin (gray) (Deplazes et al., 2013). (j) $\delta^{18}O$ of NGRIP (black) (North Greenland Ice Core Project Members, 2004; Rasmussen et al., 2014). The chronology of the OD, OD-a, and OD-b (top part) is based on the MAAT record; GI-1e, GS-2.1a, and GS-2.1b (bottom part) are based on INTIMATE chronology (Rasmussen et al., 2014). (For interpretation of the references to color in this figure legend, the reader is referred to the web version of this article.)

Downloaded from https://www.cambridge.org/core. University of Minnesota Libraries, on 25 Aug 2021 at 21:56:09, subject to the Cambridge Core terms of use, available at https://www.cambridge.org/core/terms. https://doi.org/10.1017/qua.2020.112

In that context, MAAT $\delta^{13}C$ starts a pronounced increase from 18.2 ka onward (Fig. 6b), thus establishing the beginning of the OD in this area. This continental response to stadial conditions is contemporaneous with the marine realm, with a decrease in the sea surface temperatures seen in the alkenone-based temperature record of the Iberian margin (Fig. 6f) and in the $\delta^{18}O$ of the *G. bulloides* in the Balearic Sea (Fig. 6d). The date proposed for the beginning of the OD matches the onset of the retreat of the Scandinavian ice sheet and related freshwater inputs in the North Atlantic (Toucanne et al., 2015).

The AMOC weakening occurs during 18–17.5 ka, although it was not of enough magnitude to reach a collapse or near-collapse state (Ivanovic et al., 2018). In that time interval, a gradual warming is seen in the Iberian margin (Fig. 6f), the western Mediterranean (Cacho et al., 1999, 2001), and in the subtropical North Atlantic at ~17.5 ka (Chapman et al., 1996). At the same time, widespread glacial retreats are accounted for globally (Stanford et al., 2011), regionally consistent with the high turbidite activity reported in the Iberian margin (Lebreiro et al., 2009). Tentatively, such mild conditions are marked by the excursion to lower $\delta^{13}C$ values in MAAT that peak at 17.6 ka.

Around 17 ka, lower sea surface temperatures are seen in the Iberian margin and Alborán Sea (Fig. 6e, f), and an increase of silt/clay ratio is seen in the Balearic Sea (Fig 6c), attributed to enhanced deep currents from the Gulf of Lions that are able to transport coarse material to the Minorca sediment drift (Frigola et al., 2008). These currents are associated with the degree of generation of the western Mediterranean Deep Water, a process triggered by the cool northwesterly winds that occurs mainly during winter (Sierro et al., 2005). Model simulations provide evidence for an altered atmospheric circulation regime since the last glacial maximum, characterized by a stronger, more zonally oriented Atlantic jet and reduced storminess (Li and Battisti, 2008). While the silt/clay ratio suggests a weaker western Mediterranean Deep Water since 18.2 ka, the change at ~17 ka, coeval with the trend to cold conditions, would be consistent with a southward migration of the polar jet. This hypothesis is supported by the aeolian activity reported from dune fields along the central coast of Portugal, with maximum activity peaks at 17.5 ± 1.0 ka related to the shift of the storm track toward lower latitudes (Costas et al., 2016). The cold conditions and migration of the polar jet are in agreement with the AMOC slowdown accounted at higher latitudes during that time (McManus et al., 2004; Stanford et al., 2006). Likewise, the resultant higher atmospheric pressure gradient and the southward displacement of the subtropical gyre explain enhanced westerlies (Repschläger et al., 2015). This scenario implies that a substantial amount of precipitation could be brought to Iberia by the westerlies, especially during winter (Cortesi et al., 2014). It is worth noting that the shift in the regime of the westerlies seems not to be recorded in the MAAT record; no change is observed at that time, suggesting that the rainfall source in the study area is mostly independent of the westerlies' regime. This consideration reinforces the Mediterranean influence in the present record.

The temperatures were still low at ~16.5 ka, with a chironomid-based reconstruction of a mean temperature for July of 10°C at Origlio Lake in the southern Alps, which is 10°C cooler than today (Samartin et al., 2012). The pattern of cold sea surface temperatures and a weaker western Mediterranean Deep Water lasts until the occurrence of the main discharge of icebergs during HE-1 (Fig. 6c), dated by the anomalies in the $\delta^{18}O$ of MAAT and tentatively delimitated at 16.17–15.89 ka, in agreement with the timing in the Ostolo record (Fig. 4). Two main discharges of IRD were identified in the Iberian margin during HS-1; the first occurred at ~17.5–17 ka, whereas the second spike of larger intensity was found at ~16 ka (Fig. 6g). Similarly, iceberg discharges in the Bay of Biscay are distributed between 17 and 16 ka (Fig. 6g). In general, the flux of icebergs is much lower in this area compared with other locations such as the IRD belt (Bard et al., 2000; McManus et al., 2004). In addition, it is worth noting the different origins of the IRD between the episodes of discharges, as was interpreted from the analysis of the debris and its different magnetic susceptibility peaks (Thouveny et al., 2004). The old peak of IRD at ~17.5 ka is mainly composed of detrital carbonates, whereas the main peak at ~16 ka is composed of haematite-coated grains, suggesting a Laurentide origin for the former and a European origin for the latter (Bard et al., 2000). Recently, Hodell et al. (2017) suggested a younger age for the older episode of discharges identified in Bard et al. (2000), where reservoir ages were not properly corrected.

Heinrich events did not occur until the AMOC was at its weakest state, and subsurface temperatures were near their maximum (Marcott et al., 2011). During the main phase of IRD discharges of HE-1, the AMOC in the North Atlantic was already weakened (Fig. 6h). The large volume of melting water from the icebergs entered the Mediterranean, decreasing its salinity and reducing its thermohaline circulation in less than 1000 years (Sierro et al., 2005). Such an event might have triggered the disruption of the patterns of precipitation in eastern Iberia interpreted from the analysis of $\delta^{18}O$ frequencies (Fig. 5).

The stable signal seen in the $\delta^{13}C$ of MAAT during HE-1 that interrupted a long trend to higher values (Fig. 6b), suggesting mild conditions, coincides with a sudden warming in the Alborán Sea (approximately 4°C) and Iberian margin (Fig. 6e) and a weaker western Mediterranean Deep Water (Fig. 6c). The pattern of warming in our latitude contrasts with the cooling and sea ice expansion seen in North Atlantic higher latitudes (Hodell et al., 2017). Similar mid-Heinrich stadial warming events have been reported from the marine realm during HS-5 and HS-4, by means of sea surface temperatures in the Iberian margin and Mediterranean planktonic $\delta^{18}O$ (Skinner and Elderfield, 2007).

Modeling results suggest that the expansion of the subtropical gyre explains the warming in the North Atlantic mid-latitudes, whereas the northern North Atlantic cools due to the massive input of icebergs and meltwater (Naafs et al., 2013). Such expansion of the subtropical gyre northward during Heinrich events would be the response to the enhanced wind

Downloaded from https://www.cambridge.org/core. University of Minnesota Libraries, on 25 Aug 2021 at 21:56:09, subject to the Cambridge Core terms of use, available at https://www.cambridge.org/core/terms. https://doi.org/10.1017/qua.2020.112

stress and weakening of the subpolar gyre with the southward expansion of sea ice (Renold et al., 2010). Hence, the North Atlantic surface water exhibits a different temperature pattern during Heinrich events, with cool waters reaching the center of the IRD belt; a warming is seen at the southern end, referred to as a seesaw pattern in sea surface temperatures between mid-latitude and northern North Atlantic (Naafs et al., 2013).

Most European records infer relatively warmer conditions at ~16 ka. Stalagmites from Villars and Chauvet caves in southern France started to grow synchronously at 15.9 ± 0.5 ka, suggesting climatic conditions that favor carbonate precipitation (Genty et al., 2006). Forest expansion has been reported south of the Alps at ~16 ka (Hofstetter et al., 2006; Vescovi et al., 2007) and in Italy (Wick, 2004; Finsinger et al., 2006), suggesting afforestation more than a millennium before the Bølling period. The warm conditions at ~15.9–15.8 ka propagated rapidly eastward, with a reinforced Indian summer monsoon (Lechleitner et al., 2017) and eastern Asia summer monsoon (Wang et al., 2001; Cheng et al., 2009). In contrast, this warming has not been reported in sequences from the northern Alps (von Grafenstein et al., 1999), suggesting that the afforestation in that area did not start before the Bølling period (Litt et al., 2001).

The last episode of ice sheet retreat of the deglaciation in Europe was recorded from 16 to 14 ka (Toucanne et al., 2008). The gradual trend during this period, as seen in lower $\delta^{18}O$ and $\delta^{13}C$ values in MAAT, coincides with a warming of sea surface temperatures from the Iberian margin (Fig. 6f), akin to the tropical Atlantic pattern inferred from the Cariaco basin sediment record (Fig. 6i). In contrast, the Mediterranean exhibits a cessation of gradual warming at ~15.6 ka, as recorded in the Alborán and Balearic Seas, with cold conditions that lasted until the onset of the Bølling (Fig. 6d, e). During that time, the AMOC keeps being disrupted (Fig. 6g), and its resumption coincides with the Bølling warming rather than with the end of the iceberg discharges (Stanford et al., 2011). Similarly, Greenland ice cores exhibit cold conditions during the same time, a trend that starts declining at ~15.2 ka until the sharp increase in temperature that occurs at 14.7 ka (Fig. 6j).

CONCLUSIONS

This study presents the first speleothem from Europe that records vegetation changes and rainfall patterns during the full duration of the OD, the counterpart of HS-1 in the terrestrial record. This absolute-dated record provides ages for two key events throughout the OD: (1) the onset of cold conditions that triggered the decay of vegetation dated to 18.13 ± 0.08 ka, and (2) the discharge of icebergs during HE-1, as inferred from $\delta^{18}O$ anomalies and dated from 16.17 to 15.89 ka.

The hydrological proxies of this record ($\delta^{18}O$, Mg/Ca, and Sr/Ca) and the growth rate suggest a two-step evolution throughout the OD, separated by the period when meltwater mixing occurred from 16.17 to 15.89 ka. The stages are: (1) OD-a, 18.13–16.17 ka, characterized by wet conditions and a faster growth rate; and (2) OD-b, 15.89–14.81 ka, characterized by dryness and a slower growth rate. Such release of fresh water is attributed to have somehow triggered the disruption in rainfall patterns in the eastern Iberian Peninsula during that time, as was interpreted from the cessation of multidecadal and multicentennial rainfall frequencies. Our hydrological reconstruction, characterized by relatively humid conditions in this sector during most of the OD, together with those made in other studies in northwestern and northeastern Iberia, matches the occupation of hunter-gatherers during that time, as inferred from the available archaeological sites.

ACKNOWLEDGMENTS

We acknowledge funding received from NSFC 41888101 to Cheng and Pérez-Mejías; NSF grant 1702816 to Lawrence Edwards and Cheng; and CGL2016-77479-R (SPYRIT) and CTM2016-75411-R (CHIMERA) to Moreno and Cacho, respectively. The authors would like to acknowledge the use of Servicio General de Apoyo a la Investigación-SAI, University of Zaragoza, and the help of all those involved during the field work. This is a contribution of the research groups "Procesos geoambientales y cambio global" (E02_17R) and "Geotransfer" (E32_17R and E32_20R) from the Aragón Government, Pyrenean Institute of Ecology, and University of Zaragoza. We thank the senior editor, Lewis Owen, the guest editor, Dominik Faust, and the two anonymous reviewers for the constructive comments that improved the manuscript.

REFERENCES

Ait Brahim, Y., Cheng, H., Sifeddine, A., Wassenburg, J.A., Cruz, F.W., Khodri, M., Sha, L., *et al.*, 2017. Speleothem records decadal to multidecadal hydroclimate variations in southwestern Morocco during the last millennium. *Earth and Planetary Science Letters* 476, 1–10.

Álvarez-Solas, J., Montoya, M., Ritz, C., Ramstein, G., Charbit, S., Dumas, C., Nisancioglu, K., Dokken, T., Ganopolski, A., 2011. Heinrich Event 1: an example of dynamical ice-sheet reaction to oceanic changes. *Climate of the Past* 7, 1297–1306.

Álvarez-Solas, J., Robinson, A., Montoya, M., Ritz, C., 2013. Iceberg discharges of the last glacial period driven by oceanic circulation changes. *Proceedings of the National Academy of Sciences* 110, 16350–16354.

Atsawawaranunt, K., Comas-Bru, L., Amirnezhad Mozhdehi, S., Deininger, M., Harrison, S.P., Baker, A., Boyd, M., *et al.*, 2018. The SISAL database: a global resource to document oxygen and carbon isotope records from speleothems. *Earth System Science Data* 10, 1687–1713.

Ausín, B., Hodell, D.A., Cutmore, A., Eglinton, T.I., 2020. The impact of abrupt deglacial climate variability on productivity and upwelling on the southwestern Iberian margin. *Quaternary Science Reviews* 230, 106139

Bar-Matthews, M., Ayalon, A., Kaufman, A., 2000. Timing and hydrological conditions of Sapropel events in the eastern Mediterranean, as evident from speleothems, Soreq cave, Israel. *Chemical Geology* 169, 145–156.

Bard, E., Rostek, F., Turon, J.L., Gendreau, S., 2000. Hydrological impact of Heinrich events in the subtropical northeast Atlantic. *Science* 289, 1321–1324.

Downloaded from https://www.cambridge.org/core. University of Minnesota Libraries, on 25 Aug 2021 at 21:56:09, subject to the Cambridge Core terms of use, available at https://www.cambridge.org/core/terms. https://doi.org/10.1017/qua.2020.112

Barker, S., Chen, J., Gong, X., Jonkers, L., Knorr, G., Thornalley, D., 2015. Icebergs not the trigger for North Atlantic cold events. *Nature* 520, 333–336.

Bazzicalupo, P., Maiorano, P., Girone, A., Marino, M., Combourieu-Nebout, N., Incarbona, A., 2018. High-frequency climate fluctuations over the last deglaciation in the Alboran Sea, western Mediterranean: evidence from calcareous plankton assemblages. *Palaeogeography. Palaeoclimatology, Palaeoecology* 506, 226–241.

Beaudouin, C., Jouet, G., Suc, J.-P., Berné, S., Escarguel, G., 2007. Vegetation dynamics in southern France during the last 30 ky BP in the light of marine palynology. *Quaternary Science Reviews* 26, 1037–1054.

Becker, D., Verheul, J., Zickel, M., Willmes, C., 2015. LGM Paleoenvironment of Europe: Map. https://doi.org/10.5880/SFB806.15.

Beghin, P., Charbit, S., Kageyama, M., Combourieu-Nebout, N., Hatté, C., Dumas, C., Peterschmitt, J.-Y., 2015. What drives LGM precipitation over the western Mediterranean? A study focused on the Iberian Peninsula and northern Morocco. *Climate Dynamics* 46, 2611–2631.

Bernal-Wormull, J.L., Moreno, A., Pérez-Mejías, C., Bartolomé, M., Aranburu, A., Arriolabengoa, M., Iriarte, E., *et al*., under review. Immediate temperature response in northern Iberia to last deglacial changes in the North Atlantic.

Bond, G., Showers, W., Elliot, M., Evans, M., Lotti, R., Hajdas, I., Bonani, G., Johnson, S., 1999. The North Atlantic's 1–2 kyr climate rhythm: relation to Heinrich events, Dansgaard/Oeschger cycles and the Little Ice Age. In: Alley, R.B., Clark, P.U., Keigwin, L., Webb, R. (Eds.), *Mechanisms of Global Climate Change at Millennial Time Scales*. Geophysical Monograph. American Geophysical Union, Washington DC, pp. 35–58.

Breitenbach, S.F.M., Rehfeld, K., Goswami, B., Baldini, J.U.L., Ridley, H.E., Kennett, D.J., Prufer, K.M., *et al*., 2012. Constructing proxy records from age models (COPRA). *Climate of the Past* 8, 1765–1779.

Broecker, W.S., 1994. Massive iceberg discharges as triggers for global climate change. *Nature* 372, 421–424.

Broecker, W.S., Putnam, A.E., 2012. How did the hydrologic cycle respond to the two-phase mystery interval? *Quaternary Science Reviews* 57, 17–25.

Cacho, I., Grimalt, J.O., Canals, M., Sbaffi, L., Shackleton, N.J., Schönfeld, J., Zahn, R., 2001. Variability of the western Mediterranean sea surface temperatures during the last 25,000 years and its connection with the Northern Hemisphere climatic changes. *Paleoceanography* 16, 40–52.

Cacho, I., Grimalt, J.O., Pelejero, C., Canals, M., Sierro, F.J., Flores, J.A., Shackleton, N.J., 1999. Dansgaard-Oeschger and Heinrich event imprints in Alboran Sea temperatures. *Paleoceanography* 14, 698–705.

Chapman, M.R., Shackleton, N.J., Zhao, M., Eglinton, G., 1996. Faunal and alkenone reconstructions of subtropical North Atlantic surface hydrography and paleotemperature over the last 28 kyr. *Paleoceanography* 11, 343–357.

Charles, C.D., Rind, D., Jouzel, J., Koster, R.D., Fairbanks, R.G., 1994. Glacial-interglacial changes in moisture sources for Greenland: influences on the ice core record of climate. *Science* 263, 508–511.

Cheng, H., Edwards, L.R., Hoff, J., Gallup, C.D., Richards, D.A., Asmerom, Y., 2000. The half-lives of uranium-234 and thorium-230. *Chemical Geology* 169, 17–33.

Cheng, H., Edwards, L.R., Shen, C.-C., Polyak, V.J., Asmerom, Y., Woodhead, J., Hellstrom, J., *et al*., 2013. Improvements in ^{230}Th dating, ^{230}Th and ^{234}U half-life values, and U–Th isotopic measurements by multi-collector inductively coupled plasma mass spectrometry. *Earth and Planetary Science Letters* 371–372, 82–91.

Cheng, H., Edwards, R.L., Broecker, W.S., Denton, G.H., Kong, X., Wang, Y., Zhang, R., Wang, X., 2009. Ice Age terminations. *Science* 326, 248–252.

Cheng, H., Sinha, A., Verheyden, S., Nader, F.H., Li, X.L., Zhang, P.Z., Yin, J.J., *et al*., 2015. The climate variability in northern Levant over the past 20,000 years. *Geophysical Research Letters* 42, 8641–8650.

Collatz, G.J., Berry, J.A., Clark, J.S., 1998. Effects of climate and atmospheric CO_2 partial pressure on the global distribution of C 4 grasses: present, past, and future. *Oecologia* 114, 441–454.

Columbu, A., Drysdale, R., Capron, E., Woodhead, J., De Waele, J., Sanna, L., Hellstrom, J., Bajo, P., 2017. Early last glacial intra-interstadial climate variability recorded in a Sardinian speleothem. *Quaternary Science Reviews* 169, 391–397.

Combourieu Nebout, N., Peyron, O., Dormoy, I., Desprat, S., Beaudouin, C., Kotthoff, U., Marret, F., 2009. Rapid climatic variability in the west Mediterranean during the last 25000 years from high resolution pollen data. *Climate of the Past* 5, 503–521.

Combourieu Nebout, N., Turon, J.L., Zahn, R., Capotondi, L., Londeix, L., Pahnke, K., 2002. Enhanced aridity and atmospheric high-pressure stability over the western Mediterranean during the North Atlantic cold events of the past 50 k.y. *Geology* 30, 863–866.

Cortesi, N., Gonzalez-Hidalgo, J.C., Trigo, R.M., Ramos, A.M., 2014. Weather types and spatial variability of precipitation in the Iberian Peninsula. *International Journal of Climatology* 34, 2661–2677.

Costas, S., Naughton, F., Goble, R., Renssen, H., 2016. Windiness spells in SW Europe since the last glacial maximum. *Earth and Planetary Science Letters* 436, 82–92.

Dansgaard, W., 1964. Stable isotopes in precipitation. *Tellus* 16, 436–468.

Dansgaard, W., Clausen, H.B., Gundestrup, N., Hammer, C.U., Johnsen, S.F., Kristinsdottir, P.M., Reeh, N., 1982. A new Greenland deep ice core. *Science* 218, 1273–1277.

Dansgaard, W., Johnsen, S.J., Clausen, H.B., Dahl-Jensen, D., Gundestrup, N.S., Hammer, C.U., Hvidberg, C.S., *et al*., 1993. Evidence for general instability of past climate from a 250-kyr ice-core record. *Nature* 364, 218–220.

Denton, G.H., Alley, R.B., Comer, G.C., Broecker, W.S., 2005. The role of seasonality in abrupt climate change. *Quaternary Science Reviews* 24, 1159–1182.

Denton, G.H., Anderson, R.F., Toggweiler, J.R., Edwards, R.L., Schaefer, J.M., Putnam, A.E., 2010. The last glacial termination. *Science* 328, 1652–1656.

Deplazes, G., Lückge, A., Peterson, L.C., Timmermann, A., Hamann, Y., Hughen, K.A., Röhl, U., *et al*., 2013. Links between tropical rainfall and North Atlantic climate during the last glacial period. *Nature Geoscience* 6, 213–217.

Dorale, J.A., Edwards, R.L., Ito, E., González, L.A., 1998. Climate and vegetation history of the midcontinent from 75 to 25 ka: a speleothem record from Crevice cave, Missouri, USA. *Science* 282, 1871–1874.

Drysdale, R.N., 2006. Late Holocene drought responsible for the collapse of Old World civilizations is recorded in an Italian cave flowstone. *Geology* 34, 101–104.

Drysdale, R.N., Hellstrom, J.C., Zanchetta, G., Fallick, A.E., Sanchez Goni, M.F., Couchoud, I., McDonald, J., Maas, R.,

Downloaded from https://www.cambridge.org/core. University of Minnesota Libraries, on 25 Aug 2021 at 21:56:09, subject to the Cambridge Core terms of use, available at https://www.cambridge.org/core/terms. https://doi.org/10.1017/qua.2020.112

Lohmann, G., Isola, I., 2009. Evidence for obliquity forcing of Glacial Termination II. *Science* 325, 1527–1531.

Eynaud, F., Malaizé, B., Zaragosi, S., de Vernal, A., Scourse, J., Pujol, C., Cortijo, E., *et al*., 2012. New constraints on European glacial freshwater releases to the North Atlantic Ocean. *Geophysical Research Letters* 39.

Fairchild, I.J., Borsato, A., Tooth, A.F., Frisia, S., Hawkesworth, C.J., Huang, Y.M., McDermott, F., Spiro, B., 2000. Controls on trace element (Sr-Mg) compositions of carbonate cave waters: implications for speleothem climatic records. *Chemical Geology* 166, 255–269.

Fairchild, I.J., Smith, C., Baker, A., Fuller, L., Spötl, C., Mattey, D., McDermott, F., 2006. Modification and preservation of environmental signals in speleothems. *Earth-Science Reviews* 75, 105–153.

Fairchild, I.J., Treble, P.C., 2009. Trace elements in speleothems as recorders of environmental change. *Quaternary Science Reviews* 28, 449–468.

Finsinger, W., Tinner, W., van der Knaap, W.O., Ammann, B., 2006. The expansion of hazel (*Corylus avellana L.*) in the southern Alps: a key for understanding its early Holocene history in Europe? *Quaternary Science Reviews* 25, 612–631.

Fleitmann, D., Cheng, H., Badertscher, S., Edwards, L.R., Mudelsee, M., Göktürk, O.M., Fankhauser, A., *et al*., 2009. Timing and climatic impact of Greenland interstadials recorded in stalagmites from northern Turkey. *Geophysical Research Letters* 36, 1–5.

Fletcher, W.J., Sánchez Goñi, M.F., 2008. Orbital- and sub-orbital-scale climate impacts on vegetation of the western Mediterranean basin over the last 48,000 yr. *Quaternary Research* 70, 451–464.

Fricke, H.C., O'Neil, J.R., 1999. The correlation between $^{18}O/^{16}O$ ratios of meteoric water and surface temperature: its use in investigating terrestrial climate change over geologic time. *Earth and Planetary Science Letters* 170, 181–196.

Frigola, J., Moreno, A., Cacho, I., Canals, M., Sierro, F.J., Flores, J.A., Grimalt, J.O., 2008. Evidence of abrupt changes in western Mediterranean deep water circulation during the last 50kyr: a high-resolution marine record from the Balearic Sea. *Quaternary International* 181, 88–104.

Frisia, S., 2015. Microstratigraphic logging of calcite fabrics in speleothems as tool for palaeoclimate studies. *International Journal of Speleology*. 44, 1–16.

Frisia, S., Borsato, A., Fairchild, I.J., McDermott, F., 2000. Calcite fabrics, growth mechanisms, and environments of formation in speleothems from the Italian Alps and southwestern Ireland. *Journal of Sedimentary Research* 70, 1183–1196.

Frisia, S., Borsato, A., Hellstrom, J., 2018. High spatial resolution investigation of nucleation, growth and early diagenesis in speleothems as exemplar for sedimentary carbonates. *Earth-Science Reviews* 178, 68–91.

Genty, D., Baker, A., Massault, M., Proctor, C., Gilmour, M., Pons-Branchu, E., Hamelin, B., 2001. Dead carbon in stalagmites: carbonate bedrock paleodissolution vs. ageing of soil organic matter: implications for ^{13}C variations in speleothems. *Geochimica et Cosmochimica Acta* 65, 3443–3457.

Genty, D., Blamart, D., Ghaleb, B., Plagnes, V., Causse, Ch., Bakalowicz, M., Zouari, K., Chkir, N., Hellstrom, J., Wainer, K., 2006. Timing and dynamics of the last deglaciation from European and North African $\delta^{13}C$ stalagmite profiles: comparison with Chinese and South Hemisphere stalagmites. *Quaternary Science Reviews* 25, 2118–2142.

Genty, D., Combourieu-Nebout, N., Peyron, O., Blamart, D., Wainer, K., Mansuri, F., Ghaleb, B., *et al*., 2010. Isotopic characterization of rapid climatic events during OIS3 and OIS4 in Villars cave stalagmites (SW-France) and correlation with Atlantic and Mediterranean pollen records. *Quaternary Science Reviews* 29, 2799–2820.

González-Sampériz, P., Valero-Garcés, B.L., Moreno, A., Jalut, G., García-Ruiz, J.M., Martí-Bono, C., Delgado-Huertas, A., Navas, A., Otto, T., Dedoubat, J.J., 2006. Climate variability in the Spanish Pyrenees during the last 30,000 yr revealed by the El Portalet sequence. *Quaternary Research* 66, 38–52.

Grinsted, A., Moore, J.C., Jevrejeva, S., 2004. Application of the cross wavelet transform and wavelet coherence to geophysical time series. *Nonlinear Processes in Geophysics* 11, 561–566.

Hall, I.R., Moran, S.B., Zahn, R., Knutz, P.C., Shen, C.-C., Edwards, R.L., 2006. Accelerated drawdown of meridional overturning in the late-glacial Atlantic triggered by transient pre-H event freshwater perturbation. *Geophysical Research Letters* 33, L16616.

Heinrich, H., 1988. Origin and consequences of cyclic ice rafting in the northeast Atlantic Ocean during the past 130.000 years. *Quaternary Research* 29, 142–152.

Hemming, S.R., 2004. Heinrich events: massive late Pleistocene detritus layers of the North Atlantic and their global imprint. *Reviews of Geophysics* 42, 1–43.

Hodell, D.A., Nicholl, J.A., Bontognali, T.R.R., Danino, S., Dorador, J., Dowdeswell, J.A., Einsle, J., *et al*., 2017. Anatomy of Heinrich Layer 1 and its role in the last deglaciation. *Paleoceanography* 32, 284–303.

Hofstetter, S., Tinner, W., Valsecchi, V., Carraro, G., Conedera, M., 2006. Late glacial and Holocene vegetation history in the Insubrian southern Alps: new indications from a small-scale site. *Vegetation History and Archaeobotany* 15, 87–98.

Ivanovic, R.F., Gregoire, L.J., Burke, A., Wickert, A.D., Valdes, P.J., Ng, H.C., Robinson, L.F., *et al*., 2018. Acceleration of northern ice sheet melt induces AMOC slowdown and northern cooling in simulations of the early last deglaciation. *Paleoceanography and Paleoclimatology* 33, 807–824.

Jalut, G., Turu i Michels, V., Dedoubat, J.-J., Otto, T., Ezquerra, J., Fontugne, M., Belet, J.M., *et al*., 2010. Palaeoenvironmental studies in NW Iberia (Cantabrian range): vegetation history and synthetic approach of the last deglaciation phases in the western Mediterranean. *Palaeogeography, Palaeoclimatology, Palaeoecology* 297, 330–350.

Johnson, K.R., Hu, C., Belshaw, N.S., Henderson, G.M., 2006. Seasonal trace-element and stable-isotope variations in a Chinese speleothem: the potential for high resolution paleomonsoon reconstruction. *Earth and Planetary Science Letters* 244, 394–407.

Kageyama, M., Combourieu Nebout, N., Sepulchre, P., Peyron, O., Krinner, G., Ramstein, G., Cazet, J.-P., 2005. The last glacial maximum and Heinrich Event 1 in terms of climate and vegetation around the Alboran Sea: a preliminary model-data comparison. *Comptes Rendus Geoscience* 337, 983–992.

Kim, S.-T., O'Neil, J.R., 1997. Equilibrium and nonequilibrium oxygen isotope effects in synthetic carbonates. *Geochimica et Cosmochimica Acta* 61, 3461–3475.

Lachniet, M.S., 2009. Climatic and environmental controls on speleothem oxygen-isotope values. *Quaternary Science Reviews* 28, 412–432.

Lebreiro, S.M., Voelker, A.H.L., Vizcaino, A., Abrantes, F.G., Alt-Epping, U., Jung, S., Thouveny, N., Gràcia, E., 2009.

Downloaded from https://www.cambridge.org/core. University of Minnesota Libraries, on 25 Aug 2021 at 21:56:09, subject to the Cambridge Core terms of use, available at https://www.cambridge.org/core/terms. https://doi.org/10.1017/qua.2020.112

Sediment instability on the Portuguese continental margin under abrupt glacial climate changes (last 60 kyr). *Quaternary Science Reviews* 28, 3211–3223.

Lechleitner, F.A., Amirnezhad-Mozhdehi, S., Columbu, A., Comas-Bru, L., Labuhn, I., Pérez-Mejías, C., Rehfeld, K., 2018. The potential of speleothems from western Europe as recorders of regional climate: a critical assessment of the SISAL database. *Quaternary* 1, 30.

Lechleitner, F.A., Breitenbach, S.F.M., Cheng, H., Plessen, B., Rehfeld, K., Goswami, B., Marwan, N., Eroglu, D., Adkins, J., Haug, G., 2017. Climatic and in-cave influences on $\delta^{18}O$ and $\delta^{13}C$ in a stalagmite from northeastern India through the last deglaciation. *Quaternary Research* 88, 458–471.

Li, C., Battisti, D.S., 2008. Reduced Atlantic storminess during last glacial maximum: evidence from a coupled climate model. *Journal of Climate* 21, 3561–3579.

Litt, T., Brauer, A., Goslar, T., Merkt, J., Balaga, K., Müller, H., Ralska-Jasiewiczowa, M., Stebich, M., Negendank, J.F.W., 2001. Correlation and synchronisation of late glacial continental sequences in northern central Europe based on annually laminated lacustrine sediments. *Quaternary Science Reviews* 20, 1233–1249.

Ludwig, P., Shao, Y., Kehl, M., Weniger, G.-C., 2018. The last glacial maximum and Heinrich Event I on the Iberian Peninsula: a regional climate modelling study for understanding human settlement patterns. *Global and Planetary Change* 170, 34–47.

Marcott, S.A., Clark, P.U., Padman, L., Klinkhammer, G.P., Springer, S.R., Liu, Z., Otto-Bliesner, B.L., *et al*., 2011. Ice-shelf collapse from subsurface warming as a trigger for Heinrich events. *Proceedings of the National Academy of Sciences* 108, 13415–13419.

Martin-Vide, J., Lopez-Bustins, J.-A., 2006. The western Mediterranean oscillation and rainfall in the Iberian Peninsula. *International Journal of Climatology* 26, 1455–1475.

Martrat, B., Grimalt, J.O., Shackleton, N., de Abreu, L., Hutterli, M.A., Stocker, T.F., 2007. Four climate cycles of recurring deep and surface water destabilizations on the Iberian margin. *Science* 317, 502–507.

Martrat, B., Jimenez-Amat, P., Zahn, R., Grimalt, J.O., 2014. Similarities and dissimilarities between the last two deglaciations and interglaciations in the North Atlantic region. *Quaternary Science Reviews* 99, 122–134.

McManus, J., Francois, R., Gherardi, J.M., Keigwin, L., Brown-Leger, S., 2004. Collapse and rapid resumption of Atlantic meridional circulation linked to deglacial climate changes. *Nature* 428, 834–837.

Mickler, P.J., Stern, L.A., Banner, J.L., 2006. Large kinetic isotope effects in modern speleothems. *Geological Society of America Bulletin* 118, 65–81.

Millet, L., Rius, D., Galop, D., Heiri, O., Brooks, S.J., 2012. Chironomid-based reconstruction of late glacial summer temperatures from the Ech palaeolake record (French western Pyrenees). *Palaeogeography, Palaeoclimatology, Palaeoecology* 315–316, 86–99.

Morellón, M., Valero-Garcés, B., Vegas-Vilarrúbia, T., González-Sampériz, P., Romero, Ó., Delgado-Huertas, A., Mata, P., Moreno, A., Rico, M., Corella, J.P., 2009. Late glacial and Holocene palaeohydrology in the western Mediterranean region: the Lake Estanya record (NE Spain). *Quaternary Science Reviews* 28, 2582–2599.

Moreno, A., Cacho, I., Canals, M., Prins, M.A., Sánchez Goñi, M.F., Grimalt, J.O., Weltje, G.J., 2002. Saharan dust transport and high latitude glacial climatic variability: the Alboran Sea record. *Quaternary Research* 58, 318–328.

Moreno, A., González-Sampériz, P., Morellón, M., Valero-Garcés, B.L., Fletcher, W.J., 2012. Northern Iberian abrupt climate change dynamics during the last glacial cycle: a view from lacustrine sediments. *Quaternary Science Reviews* 36, 139–153.

Moreno, A., Pérez-Mejías, C., Bartolomé, M., Sancho, C., Cacho, I., Stoll, H., Delgado-Huertas, A., Hellstrom, J., Edwards, R.L., Cheng, H., 2017. New speleothem data from Molinos and Ejulve caves reveal Holocene hydrological variability in northeast Iberia. *Quaternary Research* 88, 223–233.

Moreno, A., Stoll, H., Jiménez-Sánchez, M., Cacho, I., Valero-Garcés, B., Ito, E., Edwards, R.L., 2010. A speleothem record of glacial (25–11.6kyr BP) rapid climatic changes from northern Iberian Peninsula. *Global and Planetary Change* 71, 218–231.

Naafs, B.D.A., Hefter, J., Grützner, J., Stein, R., 2013. Warming of surface waters in the mid-latitude North Atlantic during Heinrich events. *Paleoceanography* 28, 153–163.

Naughton, F., Sánchez Goñi, M.F., Desprat, S., Turon, J.L., Duprat, J., Malaize, B., Joli, C., Cortijo, E., Drago, T., Freitas, M.C., 2007. Present-day and past (last 25 000 years) marine pollen signal off western Iberia. *Marine Micropaleontology* 62, 91–114.

Naughton, F., Sánchez Goñi, M.F., Kageyama, M., Bard, E., Duprat, J., Cortijo, E., Desprat, S., *et al*., 2009. Wet to dry climatic trend in north-western Iberia within Heinrich events. *Earth and Planetary Science Letters* 284, 329–342.

Naughton, F., Sanchez Goñi, M.F., Rodrigues, T., Salgueiro, E., Costas, S., Desprat, S., Duprat, J., *et al*., 2016. Climate variability across the last deglaciation in NW Iberia and its margin. *Quaternary International* 414, 9–22.

Ng, H.C., Robinson, L.F., McManus, J.F., Mohamed, K.J., Jacobel, A.W., Ivanovic, R.F., Gregoire, L.J., Chen, T., 2018. Coherent deglacial changes in western Atlantic Ocean circulation. *Nature Communications* 9, 2947.

North Greenland Ice Core Project Members, 2004. High-resolution record of Northern Hemisphere climate extending into the last interglacial period. *Nature* 431, 147–151.

Ortiz, J.E., Torres, T., Delgado, A., Llamas, J.F., Soler, V., Valle, M., Julià, R., Moreno, L., Díaz-Bautista, A., 2010. Palaeoenvironmental changes in the Padul basin (Granada, Spain) over the last 1 Ma based on the biomarker content. *Palaeogeography, Palaeoclimatology, Palaeoecology* 298, 286–299.

Paillard, D., Labeyrie, L., 1994. Role of the thermohaline circulation in the abrupt warming after Heinrich events. *Nature* 372, 162–164.

Palacios, D., de Andrés, N., Gómez-Ortiz, A., García-Ruiz, J.M., 2017a. Evidence of glacial activity during the Oldest Dryas in the mountains of Spain. *Geological Society, London, Special Publications* 433, 87–110.

Palacios, D., García-Ruiz, J.M., Andrés, N., Schimmelpfennig, I., Campos, N., Léanni, L., Aumaître, G., Bourlès, D.L., Keddadouche, K., 2017b. Deglaciation in the central Pyrenees during the Pleistocene–Holocene transition: timing and geomorphological significance. *Quaternary Science Reviews* 162, 111–127.

Pérez-Mejías, C., Moreno, A., Sancho, C., Bartolomé, M., Stoll, H., Cacho, I., Cheng, H., Edwards, R.L., 2017. Abrupt climate changes during Termination III in southern Europe. *Proceedings of the National Academy of Sciences* 114, 10047–10052.

Pérez-Mejías, C., Moreno, A., Sancho, C., Bartolomé, M., Stoll, H., Osácar, M.C., Cacho, I., Delgado-Huertas, A., 2018.

Downloaded from https://www.cambridge.org/core. University of Minnesota Libraries, on 25 Aug 2021 at 21:56:09, subject to the Cambridge Core terms of use, available at https://www.cambridge.org/core/terms. https://doi.org/10.1017/qua.2020.112

Transference of isotopic signal from rainfall to dripwaters and farmed calcite in Mediterranean semi-arid karst. *Geochimica et Cosmochimica. Acta* 243, 66–98.

Pérez-Mejías, C., Moreno, A., Sancho, C., Martín-García, R., Spötl, C., Cacho, I., Cheng, H., Edwards, R.L., 2019. Orbital-to-millennial scale climate variability during Marine Isotope Stages 5 to 3 in northeast Iberia. *Quaternary Science Reviews* 224, 105946.

Rahmstorf, S., 1994. Rapid climate transitions in a coupled ocean–atmosphere model. *Nature* 372, 82–85.

Rasmussen, S.O., Bigler, M., Blockley, S.P., Blunier, T., Buchardt, S.L., Clausen, H.B., Cvijanovic, I., *et al*., 2014. A stratigraphic framework for abrupt climatic changes during the last glacial period based on three synchronized Greenland ice-core records: refining and extending the INTIMATE event stratigraphy. *Quaternary Science Reviews* 106, 14–28.

Regattieri, E., Zanchetta, G., Isola, I., Bajo, P., Perchiazzi, N., Drysdale, R.N., Boschi, C., Hellstrom, J.C., Francke, A., Wagner, B., 2018. A MIS 9/MIS 8 speleothem record of hydrological variability from Macedonia (F.Y.R.O.M.). *Global and Planetary Change* 162, 39–52.

Renold, M., Raible, C.C., Yoshimori, M., Stocker, T.F., 2010. Simulated resumption of the North Atlantic meridional overturning circulation: slow basin-wide advection and abrupt local convection. *Quaternary Science Reviews* 29, 101–112.

Repschläger, J., Weinelt, M., Kinkel, H., Andersen, N., Garbe-Schönberg, D., Schwab, C., 2015. Response of the subtropical North Atlantic surface hydrography on deglacial and Holocene AMOC changes. *Paleoceanography* 30, 456–476.

Roche, D., Paillard, D., Cortijo, E., 2004. Constraints on the duration and freshwater release of Heinrich Event 4 through isotope modelling. *Nature* 432, 379–382.

Rodríguez-Arévalo, J., Díaz-Teijeiro, M.F., Castaño, S., 2011. Modelling and mapping oxygen-18 isotope composition of precipitation in Spain for hydrologic and climatic applications. In: *Isotopes in Hydrology, Marine Ecosystems and Climate Change Studies*, Vol. 1. International Atomic Energy Agency, Monaco, pp. 171–177.

Roucoux, K.H., de Abreu, L., Shackleton, N.J., Tzedakis, C., 2005. The response of NW Iberian vegetation to North Atlantic climate oscillations during the last 65 kyr. *Quaternary Science Reviews* 24, 1637–1653.

Rozanski, K., Araguás-Araguás, L., Gonfiantini, R., 1993. Isotopic patterns in modern global precipitation. In: Swart, P.K, Lohmann, K.C., Mckenzie, J., Savin, S. (Eds.), *Climate Change in Continental Isotopic Records*. Geophysical Monograph Series 78, pp. 1–36.

Samartin, S., Heiri, O., Lotter, A.F., Tinner, W., 2012. Climate warming and vegetation response after Heinrich Event 1 (16 700–16 000 cal yr BP) in Europe south of the Alps. *Climate of the Past* 8, 1913–1927.

Sánchez Goñi, M.F., Cacho, I., Turon, J., Guiot, J., Sierro, F., Peypouquet, J., Grimalt, J., Shackleton, N., 2002. Synchroneity between marine and terrestrial responses to millennial scale climatic variability during the last glacial period in the Mediterranean region. *Climate Dynamics* 19, 95–105.

Sánchez Goñi, M.F., Eynaud, F., Turon, J.L., Shackleton, N.J., 1999. High-resolution palynological record off Iberian margin: direct land-sea correlation for the last interglacial complex. *Earth and Planetary Science Letters* 171, 123–137.

Sánchez Goñi, M.F., Turon, J.L., Eynaud, F., Gendreau, S., 2000. European climatic response to millenial-scale changes in the atmosphere-ocean system during the last glacial period. *Quaternary Research* 54, 394–403.

Scholz, D., Frisia, S., Borsato, A., Spötl, C., Fohlmeister, J., Mudelsee, M., Miorandi, R., Mangini, A., 2012. Holocene climate variability in north-eastern Italy: potential influence of the NAO and solar activity recorded by speleothem data. *Climate of the Past* 8, 1367–1383.

Schrag, D.P., Adkins, J.F., McIntyre, K., Alexander, J.L., Hodell, D.A., Charles, C.D., McManus, J.F., 2002. The oxygen isotopic composition of seawater during the last glacial maximum. *Quaternary Science Reviews,* 21, 331–342.

Schulz, M., Mudelsee, M., 2002. REDFIT: estimating red-noise spectra directly from unevenly spaced paleoclimatic time series. *Computers & Geosciences* 28, 421–426.

Sierro, F.J., Hodell, D.A., Curtis, J.H., Flores, J.A., Reguera, I., Colmenero-Hidalgo, E., Bárcena, M.A., *et al*., 2005. Impact of iceberg melting on Mediterranean thermohaline circulation during Heinrich events. *Paleoceanography* 20, PA2019.

Skinner, L.C., Elderfield, H., 2007. Rapid fluctuations in the deep North Atlantic heat budget during the last glacial period: rapid deepwater temperature change. *Paleoceanography* 22, PA1205.

Stanford, J.D., Rohling, E.J., Bacon, S., Roberts, A.P., Grousset, F.E., Bolshaw, M., 2011. A new concept for the paleoceanographic evolution of Heinrich Event 1 in the North Atlantic. *Quaternary Science Reviews* 30, 1047–1066.

Stanford, J.D., Rohling, E.J., Hunter, S.E., Roberts, A.P., Rasmussen, S.O., Bard, E., McManus, J., Fairbanks, R.G., 2006. Timing of meltwater pulse 1a and climate responses to meltwater injections. *Paleoceanography* 21, PA4103.

Stríkis, N.M., Chiessi, C.M., Cruz, F.W., Vuille, M., Cheng, H., de Souza Barreto, E.A., Mollenhauer, G., *et al*., 2015. Timing and structure of Mega-SACZ events during Heinrich Stadial 1. *Geophysical Research Letters* 42, 5477–5484A.

Sturm, C., Vimeux, F., Krinner, G., 2007. Intraseasonal variability in South America recorded in stable water isotopes. *Journal of Geophysical Research: Atmospheres* 112, D20118.

Thouveny, N., Carcaillet, J., Moreno, E., Leduc, G., Nérini, D., 2004. Geomagnetic moment variation and paleomagnetic excursions since 400 kyr BP: a stacked record from sedimentary sequences of the Portuguese margin. *Earth and Planetary Science Letters* 219, 377–396.

Toucanne, S., Soulet, G., Freslon, N., Silva Jacinto, R., Dennielou, B., Zaragosi, S., Eynaud, F., Bourillet, J.-F., Bayon, G., 2015. Millennial-scale fluctuations of the European ice sheet at the end of the last glacial, and their potential impact on global climate. *Quaternary Science Reviews* 123, 113–133.

Toucanne, S., Zaragosi, S., Bourillet, J.F., Naughton, F., Cremer, M., Eynaud, F., Dennielou, B., 2008. Activity of the turbidite levees of the Celtic-Armorican margin (Bay of Biscay) during the last 30,000 years: imprints of the last European deglaciation and Heinrich events. *Marine Geology* 247, 84–103.

Tremaine, D.M., Froelich, P.N., Wang, Y., 2011. Speleothem calcite farmed in situ: modern calibration of $\delta^{18}O$ and $\delta^{13}C$ paleoclimate proxies in a continuously-monitored natural cave system. *Geochimica et Cosmochimica Acta* 75, 4929–4950.

Valero-Garcés, B.L., Zeroual, E., Kelts, K., 1998. Arid phases in the western Mediterranean region during the last glacial cycle reconstructed from lacustrine records. In: Benito, G., Baker, V.R., Gregory, K.J. (Eds.), *Paleohydrology and Environmental Change*, Wiley, London, pp. 67–80.

Vegas, J., Ruiz-Zapata, B., Ortiz, J.E., Galán, L., Torres, T., García-Cortés, Á., Gil-García, M.J., Pérez-González, A., Gallardo-Millán,

Downloaded from https://www.cambridge.org/core. University of Minnesota Libraries, on 25 Aug 2021 at 21:56:09, subject to the Cambridge Core terms of use, available at https://www.cambridge.org/core/terms. https://doi.org/10.1017/qua.2020.112

J.L., 2010. Identification of arid phases during the last 50 cal. ka BP from the Fuentillejo maar-lacustrine record (Campo de Calatrava volcanic field, Spain). *Journal of Quaternary Science* 25, 1051–1062.

Vescovi, E., Ravazzi, C., Arpenti, E., Finsinger, W., Pini, R., Valsecchi, V., Wick, L., Ammann, B., Tinner, W., 2007. Interactions between climate and vegetation during the late glacial period as recorded by lake and mire sediments archives in northern Italy and southern Switzerland. *Quaternary Science Reviews* 26, 1650–1669.

Voelker, A., Lebreiro, S., Schonfeld, J., Cacho, I., Erlenkeuser, H., Abrantes, F., 2006. Mediterranean outflow strengthening during Northern Hemisphere coolings: a salt source for the glacial Atlantic? *Earth and Planetary Science Letters* 245, 39–55.

von Grafenstein, U., Erlenkeuser, H., Brauer, A., Jouzel, J., Johnsen, S.J., 1999. A mid-European decadal isotope-climate record from 15,500 to 5000 years BP. *Science* 284, 1654–1657.

Wang, Y.J., Cheng, H., Edwards, R.L., An, Z., Wu, J.Y., Shen, C.C., Dorale, J.A., 2001. A high-resolution absolute-dated late Pleistocene monsoon record from Hulu cave, China. *Science* 294, 2345–2348.

Weniger, G.-C., de Andrés-Herrero, M., Bolin, V., Kehl, M., Otto, T., Potì, A., Tafelmaier, Y., 2019. Late glacial rapid climate change and human response in the westernmost Mediterranean (Iberia and Morocco). *PLOS ONE* 14, e0225049.

Wick, L., 2004. Full to lateglacial vegetation and climate change and evidence of glacial refugia in the south-eastern Alps. In: Ubera, J.L. (Ed.), XI International Palynological Congress (IPC). University of Cordoba, Granada, Spain, p. 529.

Wiedner, E., Scholz, D., Mangini, A., Polag, D., Mühlinghaus, C., Segl, M., 2008. Investigation of the stable isotope fractionation in speleothems with laboratory experiments. *Quaternary International* 187, 15–24.

Xu, D., Lu, H., Chu, G., Liu, L., Shen, C., Li, F., Wang, C., Wu, N., 2019. Synchronous 500-year oscillations of monsoon climate and human activity in northeast Asia. *Nature Communications* 10, 4105.

Zanchetta, G., Drysdale, R.N., Hellstrom, J., Fallick, A.E., Isola, I., Gagan, M.K., Pareschi, M.T., 2007. Enhanced rainfall in the western Mediterranean during deposition of sapropel S1: stalagmite evidence from Corchia cave (central Italy). *Quaternary Science Reviews* 26, 279–286.

Zaragosi, S., Eynaud, F., Pujol, C., Auffret, G.A., Turon, J.-L., Garlan, T., 2001. Initiation of the European deglaciation as recorded in the northwestern Bay of Biscay slope environments (Meriadzek terrace and Trevelyan escarpment): a multi-proxy approach. *Earth and Planetary Science Letters* 188, 493–507.

Downloaded from https://www.cambridge.org/core. University of Minnesota Libraries, on 25 Aug 2021 at 21:56:09, subject to the Cambridge Core terms of use, available at https://www.cambridge.org/core/terms. https://doi.org/10.1017/qua.2020.112